

UNCLASSIFIED

AD NUMBER
AD484625
NEW LIMITATION CHANGE
TO Approved for public release, distribution unlimited
FROM Distribution authorized to U.S. Gov't. agencies and their contractors; Critical Technology; MAY 1966. Other requests shall be referred to Naval Postgraduate School, Monterey, CA.
AUTHORITY
NPS ltr 7 Aug 1968

THIS PAGE IS UNCLASSIFIED

484625

UNITED STATES NAVAL POSTGRADUATE SCHOOL



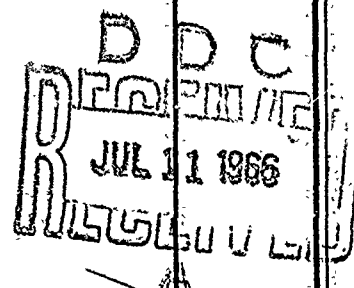
THESIS

DATA HANDLING SYSTEM IN SUPPORT
OF ANTENNA VIBRATION PROJECT

by

Ronald Hans Jesberg

May 1966



This document is subject to special export controls and each transmittal to foreign government or foreign nationals may be made only with prior approval of the U. S. Naval Postgraduate School.

DATA HANDLING SYSTEM IN SUPPORT

OF ANTENNA VIBRATION PROJECT

by

Ronald Hans Jesberg
Lieutenant, United States Navy
B.S., United States Naval Academy, 1959

Submitted in partial fulfillment
for the degree of

MASTER OF SCIENCE IN AERONAUTICAL ENGINEERING

from the

UNITED STATES NAVAL POSTGRADUATE SCHOOL
May 1966

Signature of Author *Ronald H. Jesberg*
Aeronautical Engineering Curriculum, May, 1966

Certified by *Louis V. Schmidt*

Accepted by *Richard W. Reed* Thesis Advisor
Chairman, Department of Aeronautics

Approved by *R. F. Rinehart*
Academic Dean

ABSTRACT

The low-speed bluff body studies conducted on aeroelastic models were extended by redesign of the installation in the West Coast Research Corporation's subsonic wind tunnel at the U. S. Naval Postgraduate School, Monterey, California. Improvements included stiffer support base, redesign of the spring constraint, and the use of eddy-current type displacement gages. In addition, the model's lateral response data were monitored, conditioned and recorded on one-inch magnetic tape in a voltage analog form.

The analog data were converted to digital form at a sampling rate of 500 numbers per second for a period of eight seconds per case in order to permit subsequent digital analysis in the Control Data Corporation 1604 computer. The results of this digital computation provided a numerical estimate of the spectral distribution, which gives an insight into the character of the random response of the aeroelastic structure due to the aerodynamically induced unsteady air load.

TABLE OF CONTENTS

Section	Title	Page
1.	Introduction	11
2.	Description of the Model and Equipment	15
3.	Test Procedures	23
4.	Data Processing System	25
5.	Summary	29
6.	Bibliography	30
Appendix		
A.	Wind Tunnel Surveys	40
B.	Calibration of Bently and Gulton Instruments	45
C.	Brush Oscillograph Traces of Data and Frequency Responses	48
D.	Analog to Digital Conversion System	51
E.	Power Spectral Density Program	62
F.	Definition of Auto-correlation Function and Power Spectral Densities	77

LIST OF TABLES

	Page
D-1 Program Digitize	52
D-2 Program Test	55
E-1 Power Spectral Density Computer Program	63
E-2 Subroutine Data	68
E-3 Subroutine Findit	69
E-4 Subroutine Unpack	70
E-5 Sample Computer Program Output	72

LIST OF ILLUSTRATIONS

Figure	Page
1. Schematic of Model Assembly	31
2. Scaling Parameter; Reynolds Number	32
3. Scaling Parameter; Strouhal Number	33
4. Flexure Plate	34
5. Attachment of Drill Rod to "I" Beam	34
6. Adjustable Spring Support	
A. Sliding Block in Track	35
B. Bently Displacement Gage Location	35
C. Gulton Accelerometer Location	36
7. Dynafocal Principle Support Base	36
8. Model Specifications	37
9. Complete Installation	38
10. Block Diagram of Data Acquisition System	39
 A-1 Summary of Wind Tunnel Flow Characteristics	 43
A-2 Spectrum Distribution of Hot Wire Survey	44
B-1 Calibration of Bently Inductance Measuring Device	46
B-2 Calibration of Gulton Accelerometer	47
C-1 Oscillograph Traces of Data	49
C-2 Oscillograph Traces of Frequency Responses	50

LIST OF ILLUSTRATIONS (Con't.)

	Page
D-1 Diagram of Analog to Digital Conversion System	56
D-2 Graphic Representation of Digitizing Test Tape	
A. 250 cycle per second Sine Wave	57
B. 250 cycle per second Square Wave	58
C. 250 cycle per second Triangular Wave	59
D. 20 cycle per second Band Limited White Noise	60
E. White Noise	61
E-1 Control Card For Computer Program	75
E-2 Sample Graphic Output of Power Spectral Density Program	76

TABLE OF SYMBOLS

A	- projected area = length x width
C_L	- lift/ qA = lift coefficient
C_{P_B}	- $(P_b - P_o)/q$ = coefficient of base pressure
d	- cylinder diameter, depth on square or rectangle
DC	- direct current
f	- frequency, cycles per second (cps)
l_B	- spring bar length, inches
m	- mass, slugs
P_b	- base pressure, pounds per square foot (psf)
P_o	- test section static pressure, 'psf
q	- $\rho V^2/2$ = dynamic pressure of fluid flow, psf
R	- Vd/ν = Reynolds number
RMS	- root-mean-square
$R(\tau)$	- auto-correlation function
S	- fd/v = Strouhal number
V	- velocity of undisturbed flow, feet per second (fps)
ζ	- ratio of damping to critical damping
\mathcal{F}	- Fourier transform
ρ	- density of fluid
ν	- kinematic viscosity
$\phi(\omega)$	- power spectral density
ω	- frequency, radians per second
τ	- time lag, seconds
ω_N	- natural frequency, radians per second

1. Introduction.

The use of aeroelastic type models has been widespread and is well known for estimating flutter boundaries on complete aircraft. Early airplane flutter models were primarily concerned with matching vibration frequencies, mode shapes, and mass scaling without concern for compressibility or viscosity effects. The advent of supersonic aircraft brought on an impetus to scale Mach number, hence the design and testing techniques on aeroelastic models changed in accord with the usage of transonic and supersonic wind tunnels [1]. The fairly recent importance of ground wind loads on missiles has brought emphasis upon bluff-body type aeroelastic models with similar scaling factors, except that Reynolds number is substituted for Mach number. Hence, a revision occurs in testing missile elastic models since pressurized low-speed wind tunnels are important in order to provide proper Reynolds number matching.

In addition to studying specific three-dimensional bluff bodies, a need exists for determining and evaluating both the forcing functions and structural response characteristics of idealized single degree of freedom bluff body aeroelastic models with cross-sections as a test parameter. Consistent with this type of work, a program started in 1965 by Breckon and Hite [10] has been extended and the test installation and technique has been upgraded in order to provide a better degree of insight into bluff body model response. Engineering-type improvements included a stiffer support base, redesign of the spring constraint, and the use of eddy-current type

displacement gages. These gages operate as variable inductance instruments where inductance changes are a function of air gap.

Specifically, with regard to the antenna project the horizontal members, termed boom boards, have exhibited undesirable wind induced oscillations. Ideally the boom board structure could be visualized as a constant cross-section beam having some unknown end fixity (approximately a simple support) with an evenly spaced elastic load over its length and acted upon by an unknown random aerodynamic forcing function resulting from steady wind or gusts.

The boom boards have cross sections of circular cylinders, squares, and rectangles. They all have the common feature of being bluff bodies, which means that the flow does not progress smoothly over the body, but separates from the surface in an unsteady manner which gives rise to the generation of fluctuating air loads. RMS amplitude of the response increases with increased wind velocity. The lightly damped structure acts as a band-pass filter to the random forcing function [2]. Usually the structure responds only to the forcing function centered about the resonant frequency of the structure. The principle response is essentially at the body's natural frequency.

The response of the model differs from that of the usual flutter model since bluff body response is associated with random type signals, while airplane flutter models involve harmonic type outputs. The analysis of random signals can be approached by pure analog signal processing methods where the random signal is recorded on magnetic tape and then played back through a harmonic

analyzer. Drawbacks to this technique have usually been that high quality filter circuits are needed when operating in the two cycle per second band width range; the lower limit on frequencies is between 20 and 30 cycles per second, and only power spectral density results are obtained. The auto-correlation function has not yet been obtained very satisfactorily by pure analog means.

Another technique used in handling random data is the hybrid approach; this method was utilized in this survey. The data were recorded in analog voltage form and then converted to digital form utilizing a sampling rate consistent with the frequency content of the signals. A sample rate of 500 numbers per second allows spectral distributions up to 250 cycles per second, while a digital record of eight seconds in duration provides a lower bound on spectra of about one cycle per second. The conversion to digital form utilized an analog/digital converter in conjunction with a Control Data Corporation (C.D.C.) 160 computer. Once in digital form, the binary tapes were processed through a C.D.C. 1604 computer. The output results were estimates of auto-correlation and power spectral densities.

The low-speed wind tunnel used for these investigations was readjusted and calibrated during the summer of 1965 and the flow traits were improved from those reported by Breckon and Hite [10]. Main changes included removing the flow swirl and inclination in the test section by means of corner turning vane adjustments. A five orifice yaw head was designed and constructed for this purpose and allowed measurements of flow angularity to ± 0.02 degrees.

Turbulence measurements were made in February, 1966 using a 0.0002 inch diameter tungsten hot wire probe. In addition to the usual RMS measurements, the turbulence measurements were processed through the analog to digital data handling system in order to provide a measure of the scale of turbulence and the spectral distribution of random flow eddies. Although the addition of fine mesh screens in the tunnel settling section are desirable, the tunnel in its present condition is quite usable for measurements of a character like those reported herein.

The author worked very closely with Lieutenant W. P. Mortenson throughout the entire antenna vibration survey; however, separate papers are being presented. The purpose of this paper is to specifically describe the aeroelastic model used to simulate the antenna boom boards, the data handling system utilized in data processing for the antenna vibration project, and to present the computer program for determining the power spectral density, thereby defining the response of the aero elastic wind tunnel model to the random aerodynamic forcing function. The detailed analysis and explanation of the results provided by this system and recommendations for "in the field fixes" for the antenna project can be found in [11].

The investigation was conducted by the author in conjunction with Lieutenant W. P. Mortenson during the period October 1965 through May 1966 at the U. S. Naval Postgraduate School, Monterey, California. My sincere appreciation is extended to the faculty and staff of the Aeronautical Engineering Department for their

assistance. The author is deeply indebted to Professor L. V. Schmidt for his invaluable encouragement and assistance throughout the project.

2. Description of the Model and Equipment.

In order to simulate the boom boards in the wind tunnel, it was necessary to design an aeroelastic model. The characteristics of a dynamic model are quite stringent. Ideally the model should be light weight, mounted on frictionless bearings, able to reproduce desired frequencies, and sufficiently stiff so as not to introduce undesirable structural oscillation. The general approach used was to approximate one half of the prototype by hinging the model at one end with the other end free, with controllable stiffness. Since boom boards are quite long and their end fixity conditions are close to simple supports, the first lateral vibration mode was assumed dominant. The aeroelastic model can thus be restricted to one degree of freedom in the lateral direction.

Since the intent was to observe many different configurations, interchange of the model shape was a necessity. For simplicity, it was decided to make the center of the model the strength member. An extruded aluminum "I" beam was selected primarily for its light weight and ease of machining. This aluminum beam extended the entire length of the model.

The outside configuration was formed by shaping balsa wood to the desired dimensions. The balsa covering was constructed in two symmetric pieces and contoured to fit snugly on the "I" beam (Figure 1). End plates were screwed into the balsa wood at the top and bottom; these end plates were mounted to the "I" beam by

a bracket. The end plates were adjustable to ensure that the model was centered between top and bottom of the tunnel with only a small end gap remaining.

The wind tunnel floor and ceiling were fitted with aluminum plates which had the center section recessed slightly to accept the end plates. This allowed the model to span the entire height of the tunnel and thus reduced the flow around the ends.

When scaling a dynamic model for wind tunnel testing, the variables which must be considered are: fluid density and viscosity, fluid velocity, vibration frequency, and inertia effects (stiffness, mode shapes, mass distribution, etc.). In low velocity flow the fluid may be considered incompressible, i.e., Mach number effects may be neglected.

The first lateral vibration mode has been assumed dominant, thus permitting the aeroelastic model to be restricted to one degree of freedom in the lateral direction. This allows the simplification that model inertia effects need not be scaled with respect to prototype. The remaining variables combine into the dimensionless parameters: Reynolds number ($R=vd/\nu$) and Strouhal number ($S=fd/v$).

Matching of Reynolds numbers between prototype and model assures that the aerodynamic forcing function, which causes the vibration, correspond. Matching of Reynolds number will effectively occur as far as dynamic model response is concerned when the air flow about the model is supercritical [6,7]. Matching of Strouhal

number or dimensionless frequency assures dynamic response correspondence between prototype and model [8].

To illustrate these relations a typical example follows. Assume that the prototype bluff body has a characteristic depth of 12 inches, a fundamental resonance frequency of five cps, and responds to sea level velocities of 25, 50 and 75 miles per hour.

Case	Velocity		Strouhal Number	Reynolds Number
	mph	fps		
A	25	36.7	0.136	2.34×10^5
B	50	73.3	0.068	4.66×10^5
C	75	110.0	0.046	7.00×10^5

To determine the appropriate aeroelastic model to represent the prototype, enter Figure 2 with Reynolds number (R) and model characteristic depth (d) to determine the dynamic pressure (q). With this information enter Figure 3 with q, d, Strouhal number (S) to determine the required resonance frequency of the model. Typical models which would match the above prototype condition are as follows:

Case	d	q	f _n
	inches	psf	cps
A	5.0	9.5	30
	4.0	14.4	45
B	6.0	25.2	20
	5.0	36.0	29
	4.0	57.5	45
C	6.0	57.5	20

Instead of making an exact match on both Reynolds number and Strouhal number, certain classes of bluff body cross sections may be expected to not be as severely dependent upon Reynolds number and hence only require Strouhal number matching. A clue in this direction is provided by Figures 5 and 8 of the work by Delany

and Sorensen [5] where they present steady state drag coefficient as a function of Reynolds number for several cross-section shapes. The circular cross section is well known to have a transition with respect to drag coefficient at a Reynolds number value of about 3×10^5 while square and rectangular shapes do not exhibit this trait at Reynolds numbers well in excess of 1×10^6 .

If we presume that the unsteady air loads behave in a like manner to the steady state drag coefficients, then the necessity of matching Reynolds number exactly in an aeroelastic model with a square cross section loses importance. On this assumption, the sample values considered would indicate the necessity to select model operating conditions such that Strouhal numbers of 0.05 to 0.15 corresponded to the model resonance condition for Reynolds numbers of approximately 4.0×10^5 . This condition could be matched by the model in any of the following configurations:

d=6.0 inches, $q= 18.5$ psf, $f_n=12$ to 38 cps, or
d=5.0 inches, $q= 21.7$ psf, $f_n=16$ to 48 cps, or
d=4.0 inches, $q= 42.0$ psf, $f_n=28$ to 80 cps

The top of the model, "I" beam, was attached to a rigid support by means of a flexure plate (Figure 4). This flexure plate minimized frictional damping, while allowing motion primarily in the lateral direction. Further, it provided some drag restraint. An additional drag restraint was provided near the bottom of the model by means of a stranded stainless steel cable with turnbuckle arrangement for tensioning.

The bottom of the model was supported in a manner which provided the capability of varying the model's natural frequency. A heat treated one-half inch diameter steel drill rod was attached to the aluminum "I" beam by two bolts machined to accept ball bearings. The bolts were adjustable to allow centering of the drill rod, and the ball bearings provided a relatively frictionless pin joint (Figure 5). The drill rod was cantilevered to a movable steel support block, precision drilled to accept the spring rod, and provided with six set screws which fixed the bar in position. The movable steel support block was fitted to a 16 inch precision machined wedge shaped track. Eight lag bolts secured the sliding block in any position (Figures 6 A,B,C). The track was bolted to a one-inch thick steel plate supported by four welded four-inch diameter steel pipes which formed legs in a manner similar to a dynafocal suspension principle (Figure 7). This rebuilt model support base increased the rigidity of the model's reference base over that used in [10]. The improvement in the lateral stiffness constraint provided a means for more rapid adjustment of the spring bar length while assuring that the base of the constraint was attached to the support base. Figure 8 illustrates the complete specifications of the model.

The wind tunnel utilized was the 42 inch by 60 inch subsonic tunnel located at the U. S. Naval Postgraduate School, Monterey, California. This tunnel is a closed section, vertical return, 200 mile per hour installation built by West-Coast Research Corporation of Los Angeles, California. Power is supplied by two

150 horsepower electric motors driving two independent constant speed variable pitch fans. However, for ease of operation only one fan was utilized; this fan provided adequate power for the dynamic pressure required. In addition, a survey of the dynamic pressure on tunnel centerline was completed. In order to check the turbulence level of the tunnel, a hot-wire survey was performed. The results of these surveys are presented in Appendix A. The aeroelastic model was mounted vertically in the test section as shown in Figure 9 along with an illustration of the entire data handling system.

The primary instrument for response measurement was the Bently displacement measuring device. This device provides an instantaneous measurement of the lateral displacement of the bottom of the beam.

The Bently sensor unit, a small pancake shaped coil, is excited at a one megacycle carrier frequency by a transistorized amplifier unit and power supply combination. The rapidly fluctuating magnetic field at the face of the coil allows sensing of the air gap change between the coil face and a flat non-magnetic conducting surface due to eddy current effect. The frequency limit of the Bently is 10,000 cycles per second. This is well above the 125 cycles per second anticipated during the antenna survey. In practice this device proved quite reliable with a consistent distance resolution of about 20 micro-inches. Figure 6B shows the Bently sensor unit mounted to the model support base. Therefore, the gage measured relative displacement between the support floor and the model. Appendix B provides a calibration for the Bently inductance

displacement measuring device. For test purposes, the air gap was allowed to vary in the linear range from 0.02 to 0.08 inches, where the output sensitivity was approximately 70 volts/inch.

The secondary source of model frequency response data was the Gulton type A321 accelerometer. This piezoelectric type device was used with an Endevco amplifier. The accelerometer has a flat response curve to above 3,000 cycles per second. Results of Gulton accelerometer calibrations are presented in Appendix B. It was decided to use the Bently as the primary source of data due to its reliability and ability to measure relative displacement between fixed reference and the base of the model instead of the inertial reference frame of the accelerometer (Figure 6C).

Figure 10 presents a block diagram of the entire data acquisition system. Due to the complexity of the wiring and the desire to have an orderly system, BNC fittings were used throughout in conjunction with shielded coaxial cable. The coaxial cable decreased the possibility of picking up any outside disturbances such as 60 cycle from power supplies, ground loops, and fluorescent lights.

All data were monitored and controlled through a central switch panel in a manner similar to a telephone patch panel in order to maintain a systematic control of data flow. Voltage signals from the Bently and accelerometer were monitored and recorded using a Ballantine model 320A voltmeter in order to obtain the true RMS reading of the randomly varying signal. This meter uses a diode squaring circuit so as to give an accurate measure of the RMS

voltage, and can handle situations where peak values occur up to ten times greater than the RMS.

The Vidar, integrating digital voltmeter, reads both frequency and voltage. It was utilized in the system to insure that the initial setting on the Bently, with the model stationary, was in the center of the linear range of the response characteristics of the Bently. Its secondary function was to calibrate the center frequency of the tape recorder's frequency modulating (FM) data channels.

The tape recorder/reproduce unit used was the Ampex FR-100. This provided 14 channels for the recording of data. Both frequency modulated and direct record amplifiers were available to record data. With a recorder/reproduce speed of seven and one-half inches per second, the frequency response for the frequency modulated amplifier was from zero to 1250 cycles per second. The input to the recorder was limited to one volt RMS or ± 1.40 volt peak to peak. The voltage signals from the Bently and accelerometer were recorded through the frequency modulated amplifier. Voice announcements were recorded through a direct response amplifier. These announcements properly labeled and identified the data. The system recorded the data on one inch mylar instrument grade tape so that the voltage signals which represent an analog of the model response could be analyzed at a later date.

The Tektronic 545A cathode ray oscilloscope is a single beam device which behaves in a dual beam manner using the dual trace amplifier channel, and it was used to monitor various signals.

The dual trace provided the means for simultaneously observing the signals from both the Bently and the accelerometer. Since the input to the Ampex tape recorder was limited to one volt RMS, observing the input determined whether attenuation was necessary to keep the signal within limits. Finally, the scope could be connected to the Ampex reproduce amplifier (output) to insure that the data was being properly recorded and reproduced.

3. Test Procedures.

The entire data acquisition system with a few exceptions consisted of tube elements. Therefore, prior to obtaining data, the entire system was allowed a proper warmup time in order to insure that all thermal transients had settled out. The Ampex tape recorder/reproduce amplifiers were calibrated in accordance with the operation manual.

Calibrations were recorded on the magnetic tape through the frequency modulated amplifiers on the exact channels that the Bently and acceleration voltage signals were to be recorded. This consisted of zero volts and plus and minus 1.4 volts (DC). This calibration could be utilized later during the data analysis phase.

To determine the system damping and to calibrate the spring rod length as a function of the natural frequency of the model, static tests were performed with the wind tunnel inoperative. The model base was mechanically displaced from the centered equilibrium position and sharply released. The model's decaying response of both displacement and acceleration was recorded onto magnetic tape.

The vibrational response of the model was obtained by a series of test runs. Each was run at a fixed natural frequency set by positioning the calibrated spring rod to the proper length while varying the tunnel dynamic pressure. Here again, the data from the Bently and accelerometer were recorded on one-inch magnetic tape and the RMS values from the Ballantine voltmeter were read and recorded in the data logs. Visual observations, using the Tektronic oscilloscope, were made of the response wave form to insure that the amplitude did not exceed record amplifier limitations, and further to check that data was being accurately recorded and reproduced.

Voice announcements on a separate channel preceded and followed the calibration check, model frequency response check and the dynamic data runs. This insured that the data was properly labeled and would definitely be retrievable.

The data from the one-inch magnetic tape was next played back through an analog representation of an averaging circuit and plotted to observe the continuity of the curves, and further to look for any violent or sporadic portions. As expected from the oscilloscope observations, the curves were smooth and well-behaved, although complex and random in nature. Further, it appeared that the data was a stationery random process (this was subsequently confirmed by power spectral analysis.) Since the data was well-behaved, any portion of the data could be analyzed without fear of large errors. The model frequency response check and portions of the data were

plotted on strip chart Brush oscillograph to obtain frequency.

Samples of this data may be found in Appendix C.

4. Data Processing System.

At this point, approximately 450 data runs in analog form were recorded on one-inch magnetic tape. It was desirable to form the auto-correlation function and then the power spectral density in order to obtain the response traits of the various configurations to the random forcing function. It was estimated that it would take approximately three to five man-months to process each run by hand. Obviously it was necessary to utilize the Control Data Corporation (C.D.C.) 1604 digital computer. However, a major hurdle still existed, namely the conversion of the analog data into digital form, acceptable as computer input.

The process of converting real analog data into computer digital form was accomplished in two distinct and separate steps. In the first step the analog data was digitized at discrete points and written in BIT form on one-half inch magnetic tape. The second step was to unpack the digital data and put it into a form useable in the C.D.C. 1604 as standard program input.

Figure D-1 is a block diagram of the analog to digital conversion system. The wind tunnel data from the one-inch magnetic tape was reproduced through the Electrical Engineering Department's Ampex CP-100, a solid state record/reproduce system. The digitizing computer was the CDC-160 located in the Electrical Engineering Department Computer Laboratory. The CDC-160 selects either the 12 BIT analog to digital converter unit for input, or the CDC-163

tape unit for output. The computer has a 4096 cell 12 BIT memory length. The lower 4,000 cells were reserved for storage, and the top 96 cells were reserved for programming. The core storage was an obvious limiting factor. However, 4,000 data samples were assumed adequate. The basic concept of the operation was to take samples until the core storage was full (4,000 samples) and then write this information onto one-half inch magnetic tape.

The procedure utilized a manually initiated pulse to trigger the analog to digital converter. The computer controls the inter-sample time delay and the analog to digital converter samples rapidly until 4,000 discrete samples have been taken and stored in the memory core. The computer then dumps the output onto one-half inch magnetic tape. The analog to digital converter then remains hung up until receipt of another manual pulse. Program Digitize, a CDC-160 tape program, is found in Table D-1.

A sample rate of 500 discrete points per second allows spectral distributions up to 250 cycles per second, while a digital record of eight seconds duration provides a lower bound on spectra of approximately one cycle per second. This frequency range is more than adequate since the natural frequencies of aeroelastic models tested varied from 35 to 90 cycles per second.

In order to identify each block of 4,000 data points on the tape, a 16 digit identifier was first written followed by the data points. These identifiers are extremely important since they are the only means by which the data may be retrieved at a later time. This 16 digit identifier is a manual input to Program Digitize.

The data in digital form may be recalled by subroutine Data. Subroutine Data, Table E-2, in turn uses subroutine Findit, Table E-3, which locates the identifier on the tape and subroutine Unpack, Table E-4, a machine language routine to unpack the samples so that one-to-one correlation exists between the original CDC-160 listing and the unpacked CDC 1604 version.

A short CDC-160 tape program Test, Table D-2, was used to adjust the bias voltage to minus five volts and the desired inter-sample delay to the proper time. Additional more detailed information of the digitizing system can be found in Lieutenant N. S. Barrett's thesis "Extracting Analog Signals From Noise Using The Digital Computer" [9].

In order to test the capabilities of the digitizing system, a test tape was prepared with a 250 cycle per second sine wave, square wave, triangular wave, 20 cycle per second band-limited white noise and finally white noise. The data was analyzed and presented graphically, Figures D2-6. The system worked successfully and provided very satisfactory results.

The final step in the data handling system was the computer program, written in Fortran 63, which utilized the Tukey method for estimating the power spectral density [4].

The complete program may be found in Appendix E. The program possesses sufficient comments to make it self-explanatory. However, some additional comments on the input cards are provided in Figure E-1.

Basically, this program used the data recalling system previously described. The integer format from the subroutines was converted to floating point format and converted into volts by a constant. In order to insure that no bias existed, the data were normalized to wipe out the DC term on an average basis.

The auto-correlation function of the random response was computed, and subsequently used, to estimate the spectral distribution of the energy by applying a Fourier cosine transform to the auto-correlation function. For any given signal, aperiodic or random in nature, it is quite clear that the auto-correlation function and spectral density are quite meaningful, but only the auto-correlation function is directly measurable. The power spectral density may be defined as the energy distribution on an average basis in the frequency domain; that is, energy with respect to frequency. Appendix F gives a more detailed mathematical explanation of the auto-correlation function and power spectral density to show the inter-relationships. The final step in the program was to determine the energy contained in the power spectrum by application of the trapezoidal rule. Comparing this result with the total energy provides a rapid indication of the accuracy of the results obtained. A sample listing of the data output is given in Table E-5 and is graphically presented in Figure E-2. The data and graphs specifically define the frequency response of the aeroelastic model to the aerodynamic random forcing function. This information is imperative to the investigation of the aerodynamic phenomena and subsequent analysis described in [11].

5. Summary.

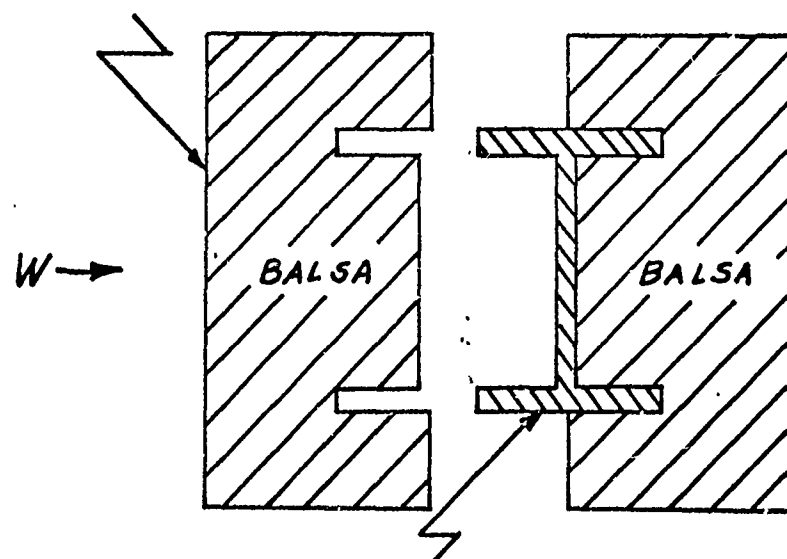
A controlled test environment for conducting wind-tunnel investigations of bluff body aeroelastic models has been established. The data acquisition and processing systems are precise, orderly, and operational. The conversion from an analog voltage record to a digital format has been accomplished with a high degree of accuracy. The computer program was utilized to analyze approximately 450 wind tunnel data runs, and presented the output in numeric and graphic form. These results were imperative to the success of the investigation and analysis of aeroelastic phenomena conducted on the various configurations as presented in [11].

BIBLIOGRAPHY

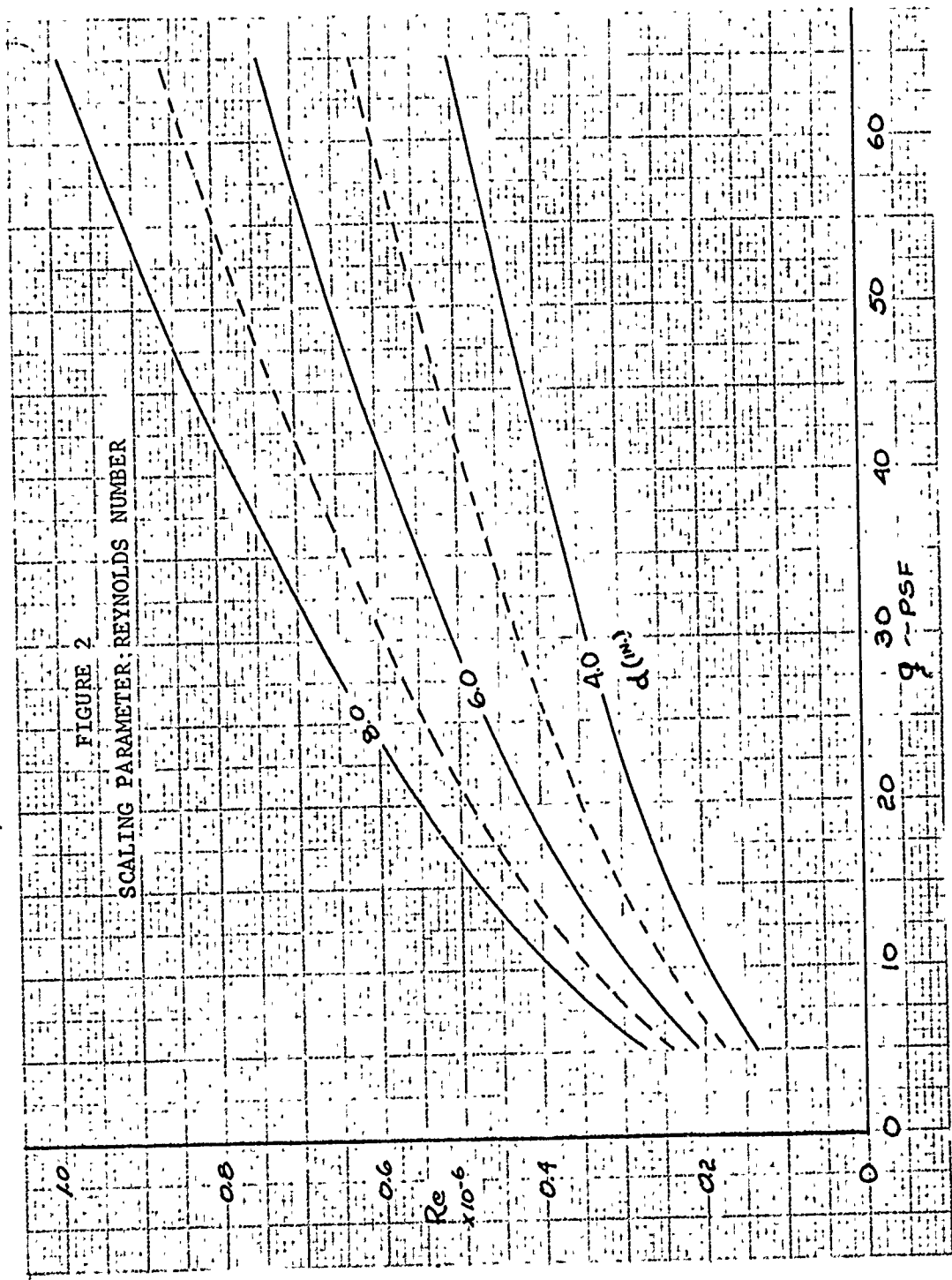
1. Bisplinghoff, R. L. and Ashley, H. Principles of Aeroelasticity. John Wiley and Sons, 1962.
2. Fung, Y. C. An Introduction to the Theory of Aeroelasticity. John Wiley and Sons, 1962.
3. Tsien, H. S.. Engineering Cybernetics. McGraw-Hill, 1954.
4. Blackman, R. B. and Tukey, J. W. The Measurement of Power Spectra. Dover, 1958
5. Delany, N. K. and Sorensen, N. E. Low-Speed Drag of Cylinders of Various Shapes. NACA TN 3038, November 1953.
6. Fung, Y. C. The Analysis of Wind-Induced Oscillations of Large and Tall Cylindrical Structures, Space Technology Laboratories, Ramo-Woolridge Corporation. 7 May 1958. Technical Report STL/TR-60-0000-09134.
7. Fung, Y. C. Fluctuating Lift and Drag Acting on a Cylinder in a Flow at Supercritical Reynolds Numbers. Space Technology Laboratories, Ramo-Woolridge Corporation. June 1960 Technical Report GM-TR-0165-00343.
8. Schmidt, L. V. Review of Dynamic Scaling for Ground Wind Load Models. Aerospace Corporation. 22 June 1964. Technical Memorandum 64(4116-42)-2.
9. Barrett, N. A. Extracting Analog Signals From Noise Using the Digital Computer. Masters Thesis U. S. Naval Postgraduate School, Monterey, California. May 1966.
10. Breckon, R. L. and Hite, P. R. Wullenwebber Antenna Vibration Study. Masters Thesis U. S. Naval Postgraduate School, Monterey, California. May 1965.
11. Mortenson, W. P. Investigation of Aeroelastic Phenomena in the Antenna Vibration Project. Engineers Thesis U. S. Naval Postgraduate School, Monterey, California. May 1966.

FIGURE 1
SCHEMATIC OF MODEL ASSEMBLY

CIRCULAR OR RECTANGULAR



3" ALUMINUM I BEAM
WITH 2" FINGERS, 1/4" THICK



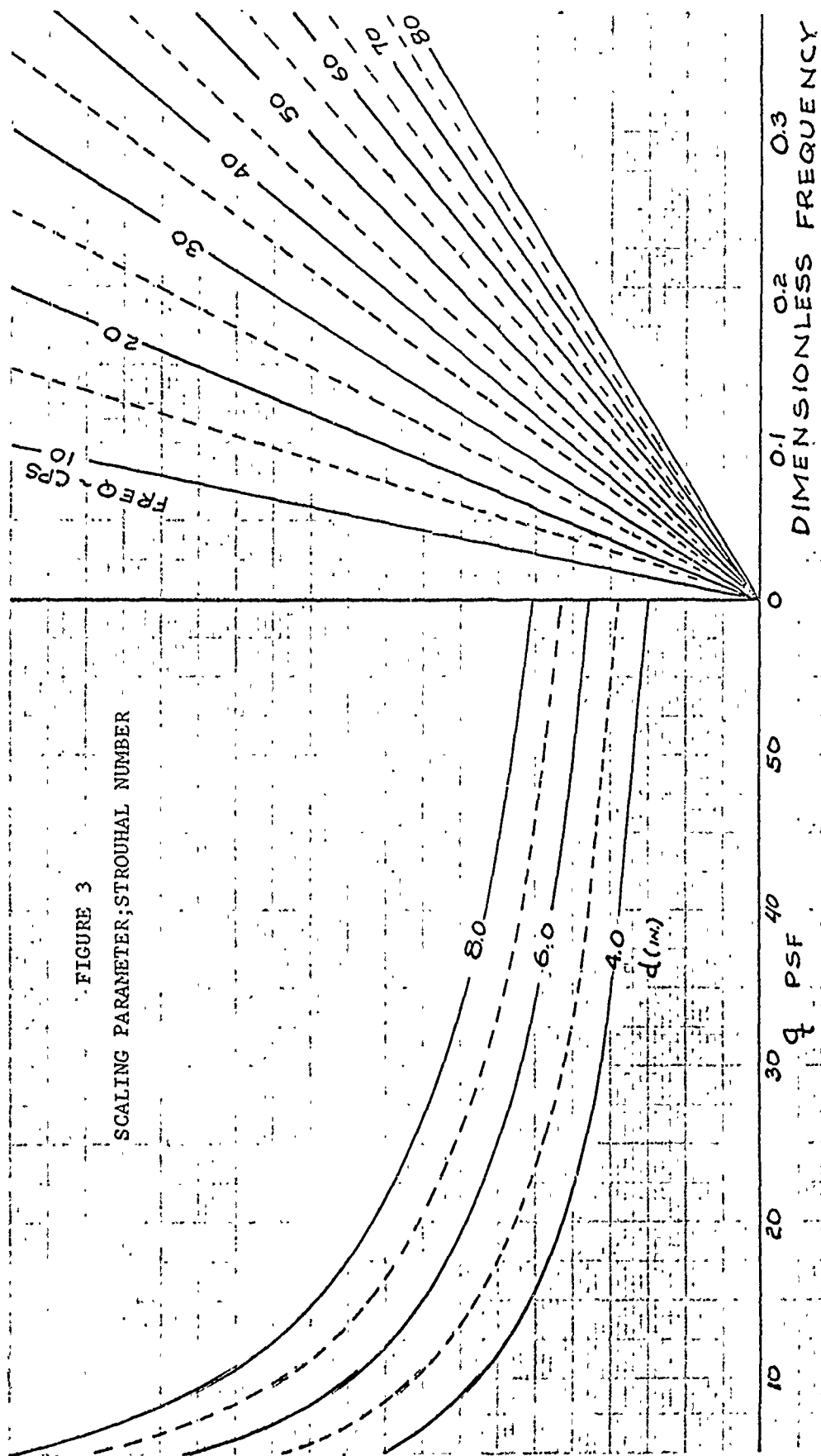


FIGURE 4
FLEXURE PLATE

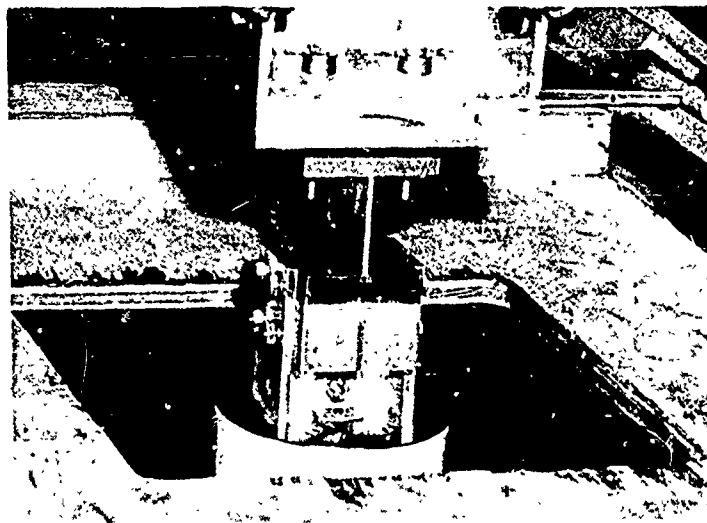


FIGURE 5
SPRING ROD JOINT

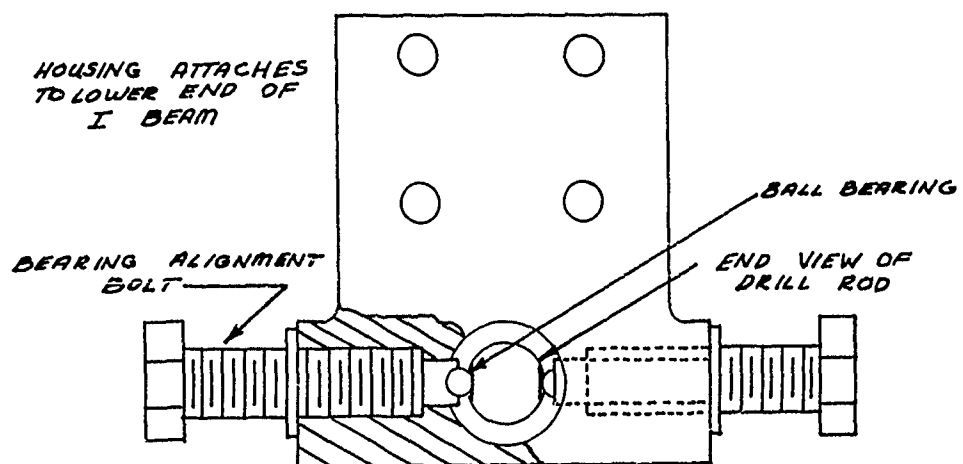


FIGURE 6A
ADJUSTABLE BLOCK

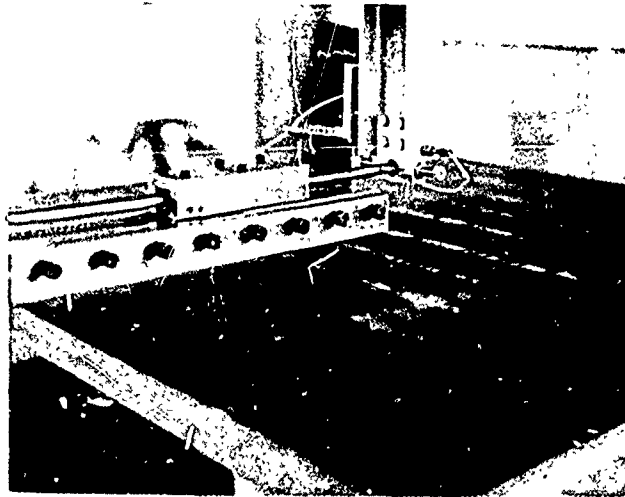


FIGURE 6B
BENTLY DISPLACEMENT GAGE

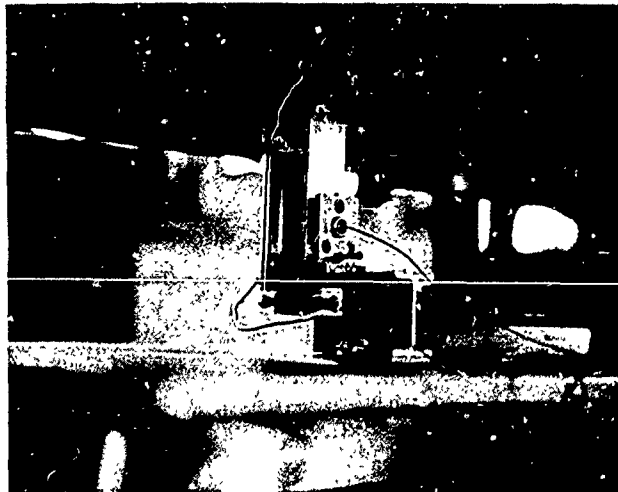


FIGURE 6C
GULTON ACCELEROMETER

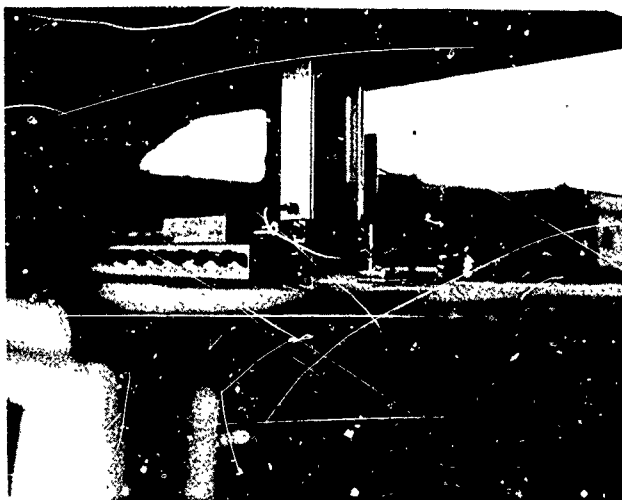
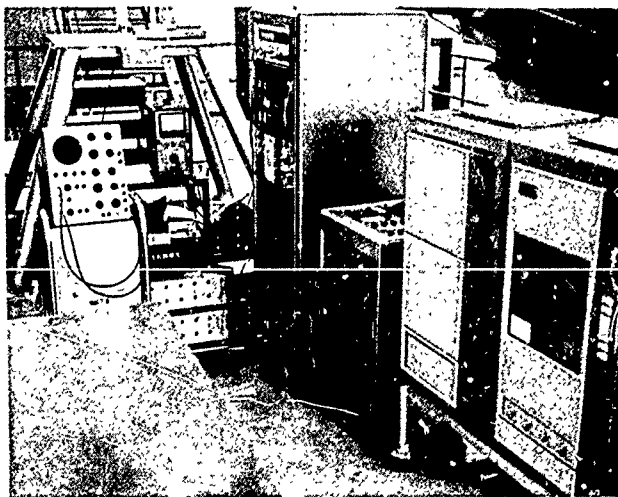


FIGURE 7
SUPPORT BASE



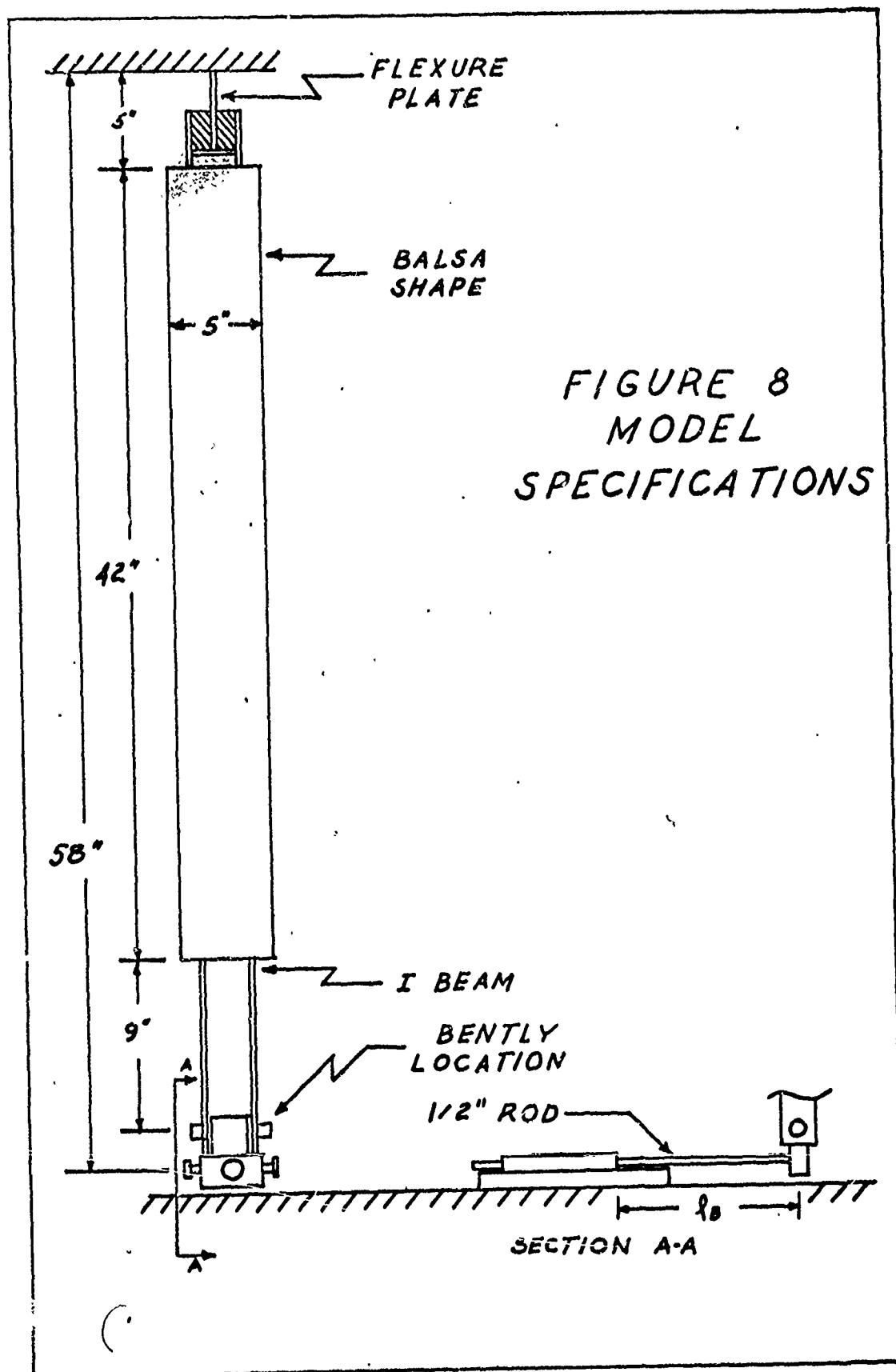


FIGURE 9
COMPLETE INSTALLATION

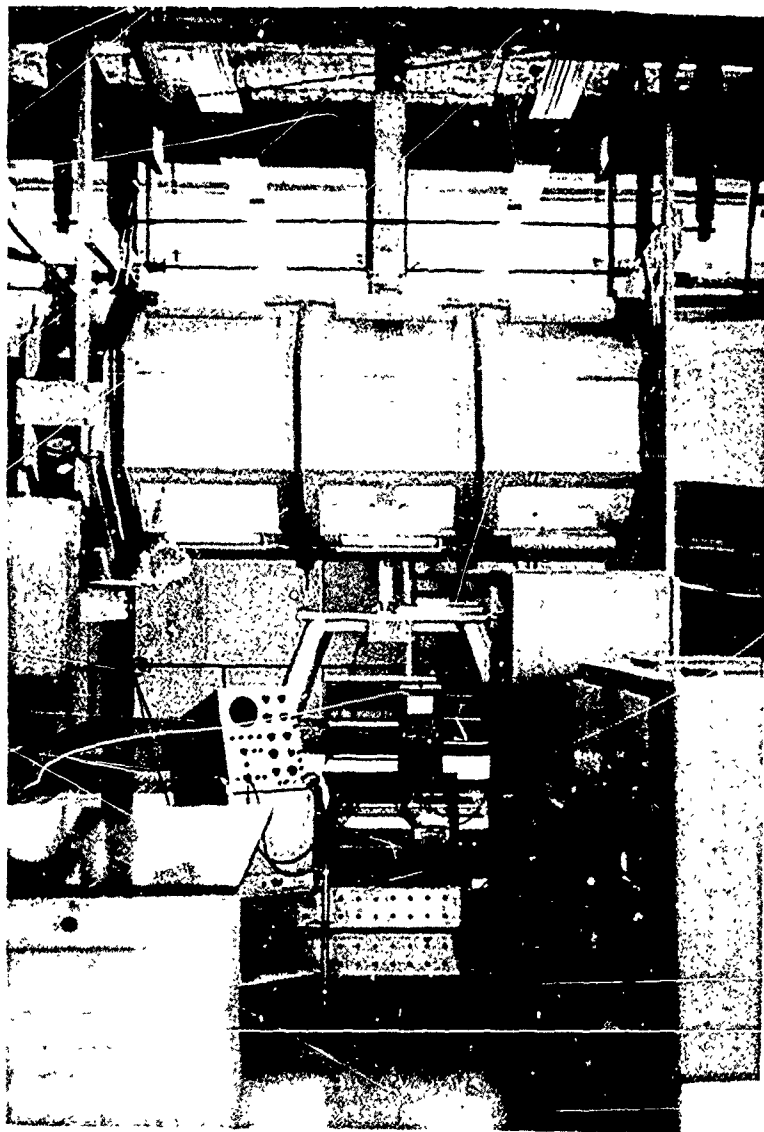
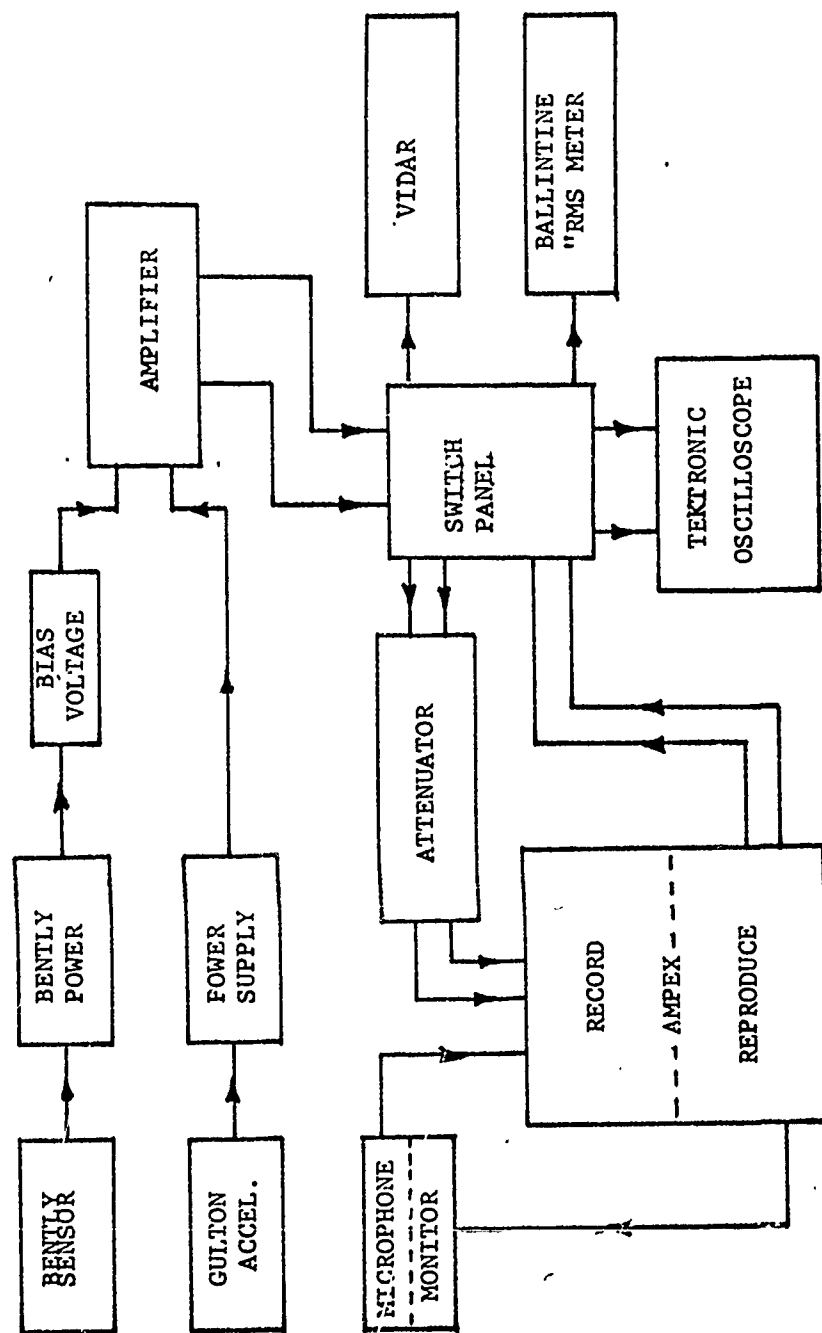


FIGURE 10
DIAGRAM OF DATA ACQUISITION SYSTEM



APPENDIX A

WIND TUNNEL TEST SECTION CALIBRATION

The test section pressure survey shown in Figure A-1 was performed at the U. S. Naval Postgraduate School's low speed wind tunnel. The profiles shown were taken 22 inches aft of the test section leading edge, with reference dynamic pressure of 40 pounds per square foot.

These wind tunnel flow traits were improved with respect to tunnel dynamic pressure and flow inclination. Although the importance of these changes upon bluff body separation may not be critical or discernible, it is good practice to have a well established and uniform test environment in the wind tunnel test section.

A constant temperature hot wire was placed on tunnel centerline at the model test station in order to make clear tunnel turbulence measurements. The hot wire was 0.001 inch diameter tungsten, approximately 0.08 inches in length and was supported on the end of two needles projecting from a support tube. It was possible to make direct measurements of turbulence level relative to free stream velocity using a prototype constant temperature amplifier circuit recently developed at the U. S. Naval Postgraduate School. These turbulence measurements were read directly by the Ballantine True RMS voltmeter, and also recorded on magnetic tape for subsequent digital analysis using procedures described elsewhere.

The direct measurements of turbulence indicated a turbulence level of approximately 0.45%, but the single wire sensed fluctuations both in the vertical and axial direction. On the assumption of isotropic turbulence, it is possible to estimate the axial velocity turbulence level as approximately 0.32%. This value was obtained uniformly for a test section q range of 10 to 40 psf. The above value of turbulence level is considered high for high calibre wind tunnel work in a low turbulence environment, but considering that no anti-turbulence screens were installed in the settling section, and that the test was concerned with bluff body separation, the value was quite acceptable. The installation of screens in the settling section should result in a much lower value of turbulence level.

The results of the digital calculations are shown on Figure A-2 with respect to both auto-correlation and power spectral density. The area of the normalized auto-correlation curve is 0.102 seconds which may be interpreted as a measure of the scale of turbulence, that is, on the average, turbulent fluctuations are unrelated for time intervals beyond 0.102 seconds. The power spectral density curve shows no dominant energy peaks other than one at 1/2 cps. It is quite possible that the 1/2 cps peak was caused by the vibration of the hot wire support. The absence of other peaks indicates an absence of noise due to fan blade rotation or an undamped flow separation from other sources in the tunnel circuit.

The basic conclusion reached from the hot wire measurements is that the test section circuit is functional in its present configuration and the addition of screens at a later date will make the facility very useful for fundamental low turbulence experiments.

The tunnel airspeed and/or dynamic pressure was set using clear tunnel values. In making a final evaluation, solid blockage effects may be taken into account. An estimate of blockage for the case of a cylinder spanning the tunnel is given by the formula:

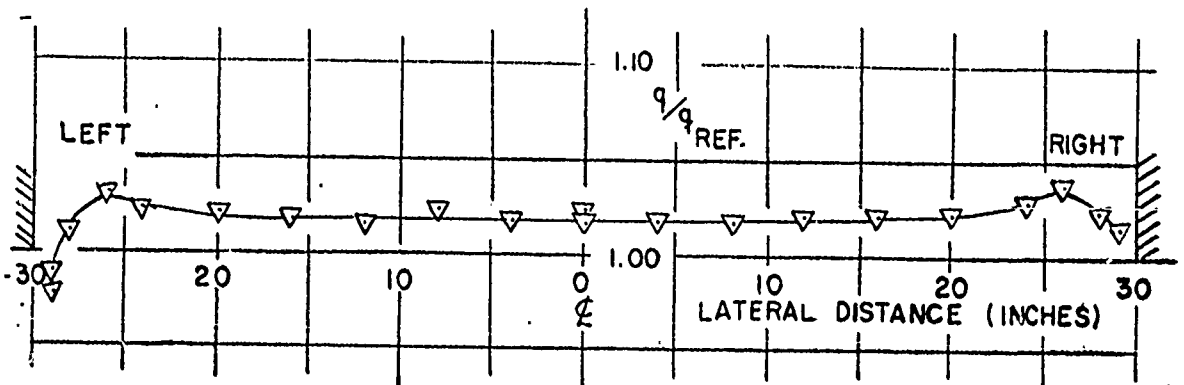
$$\epsilon_s = \frac{\pi^2 a^2}{3 h^2}$$

where a = radius of the cylinder

h = height

ϵ_s = fractional velocity increase

model width inches	ϵ_s	$q_{\text{corr}}/q_{\text{ref}}$
4	.0146	1.03
5.7	.0296	1.06
8	.0584	1.12



FLOW SURVEY
 3.5x5.0 FT. LOW SPEED WIND TUNNEL
 CLEAR TEST SECTION
 $q_{REF.} = 40$ PSF AT TEST SECTION L.E.

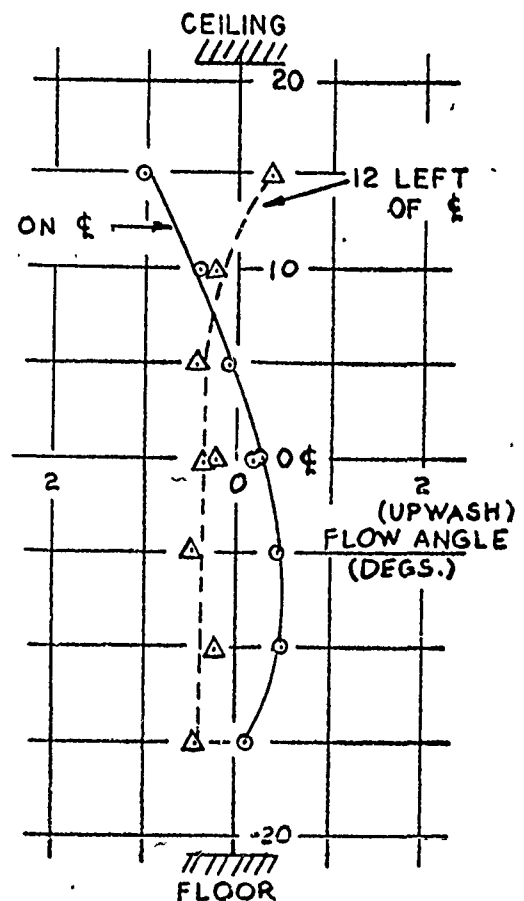
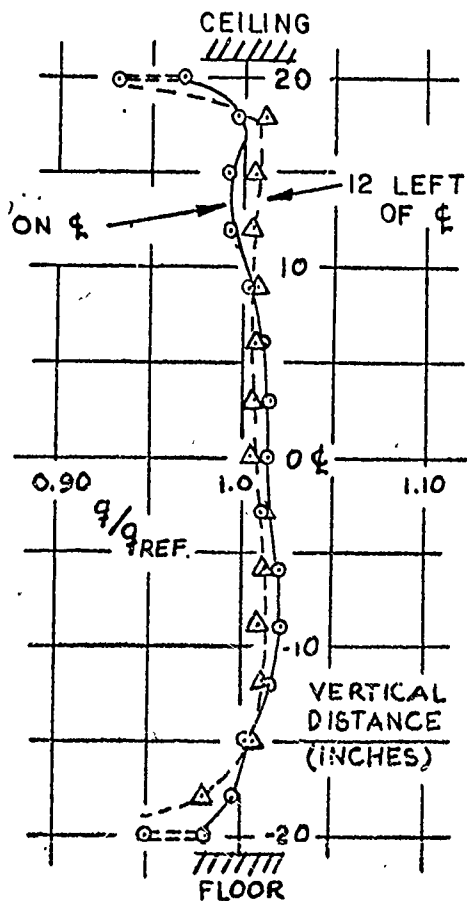
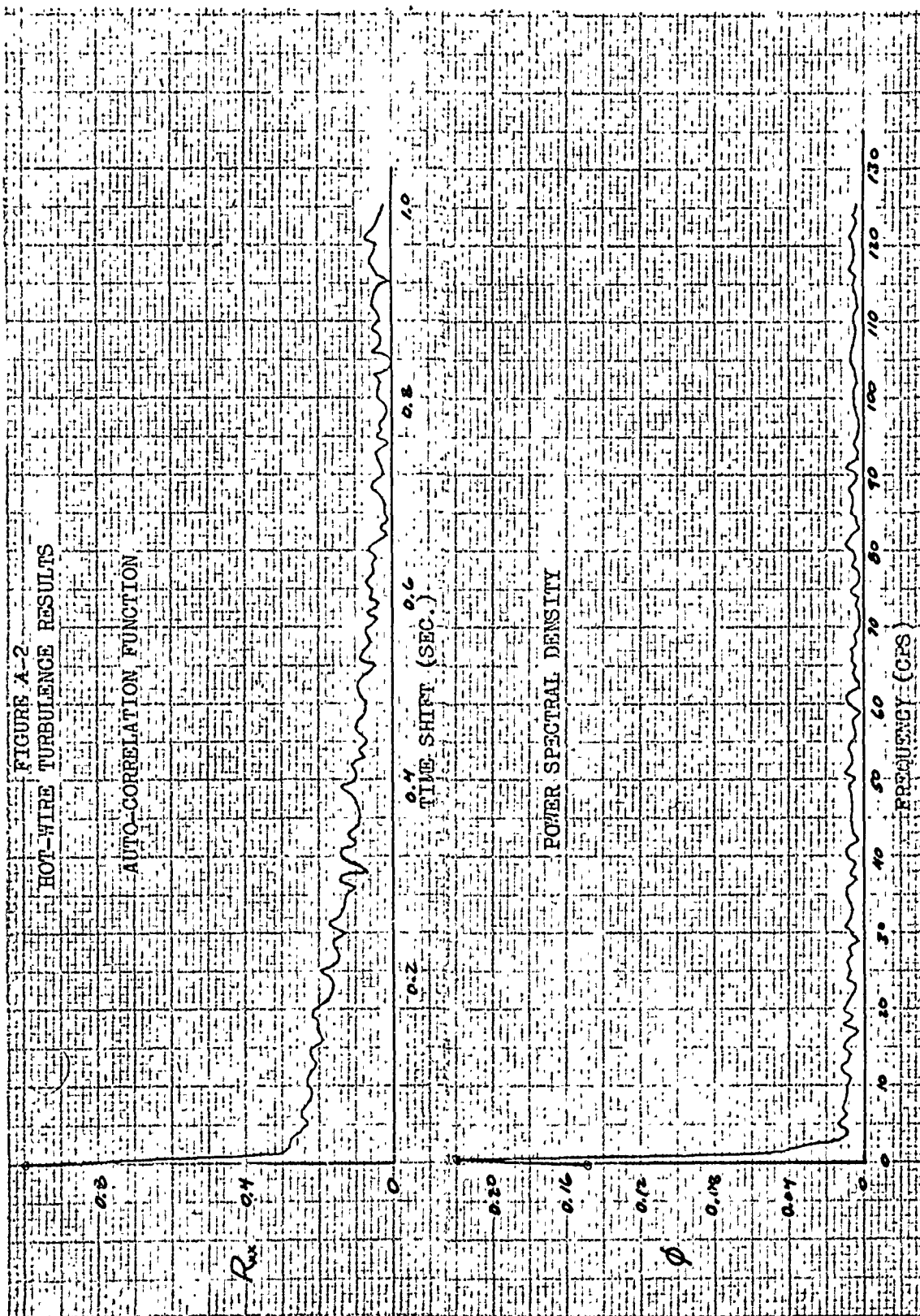


FIGURE A-1
 Summary of Wind Tunnel Flow Characteristics



APPENDIX B
CALIBRATION OF BENTLY AND GULTON INSTRUMENTS

The Bently sensor head was mounted in an aluminum test block. The procedure used was to obtain the gage voltage for a specific distance measured by a micrometer. The plot of distances versus output voltage is shown in Figure B-1. The slope of the linear region was 70 volts/inch. The Bently sensor unit was serial number 14184, and the distance detector unit model D-252 was serial number 5254. The ease of calibration and the consistent reliability made the Bently displacement measuring system an extremely useful instrument.

The Gulton model A321, a piezoelectric accelerometer, is extremely sensitive and because of its high natural frequency it can be used through a wide frequency range. However, since it is an A.C. instrument it cannot be statically calibrated. Therefore, the accelerometer was calibrated against a previously calibrated Statham on the Calidyne shaker table. The Gulton accelerometer serial number 1558 was combined with an Endevco amplifier serial number 128. The calibration is shown on Figure B-2.

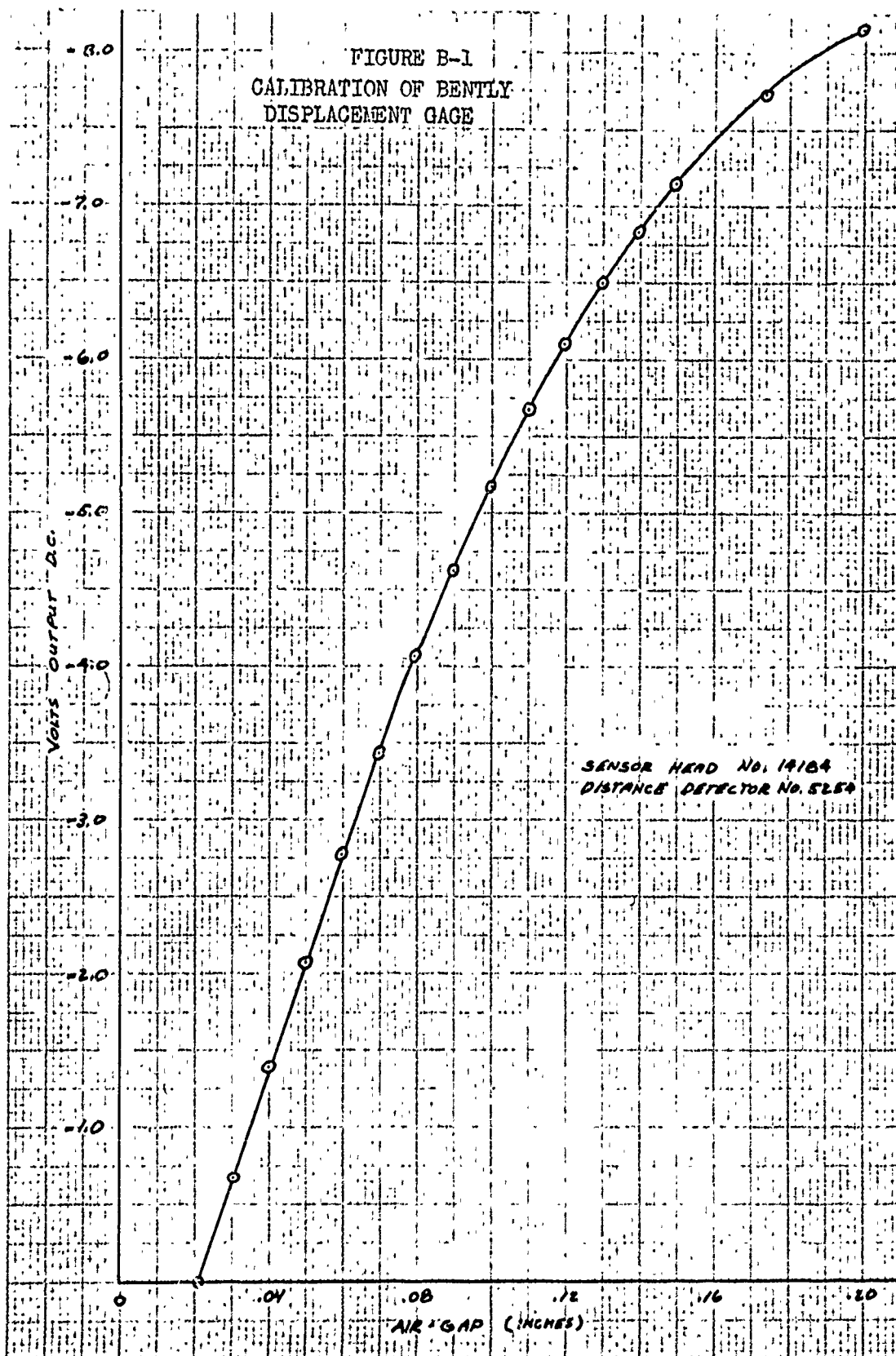
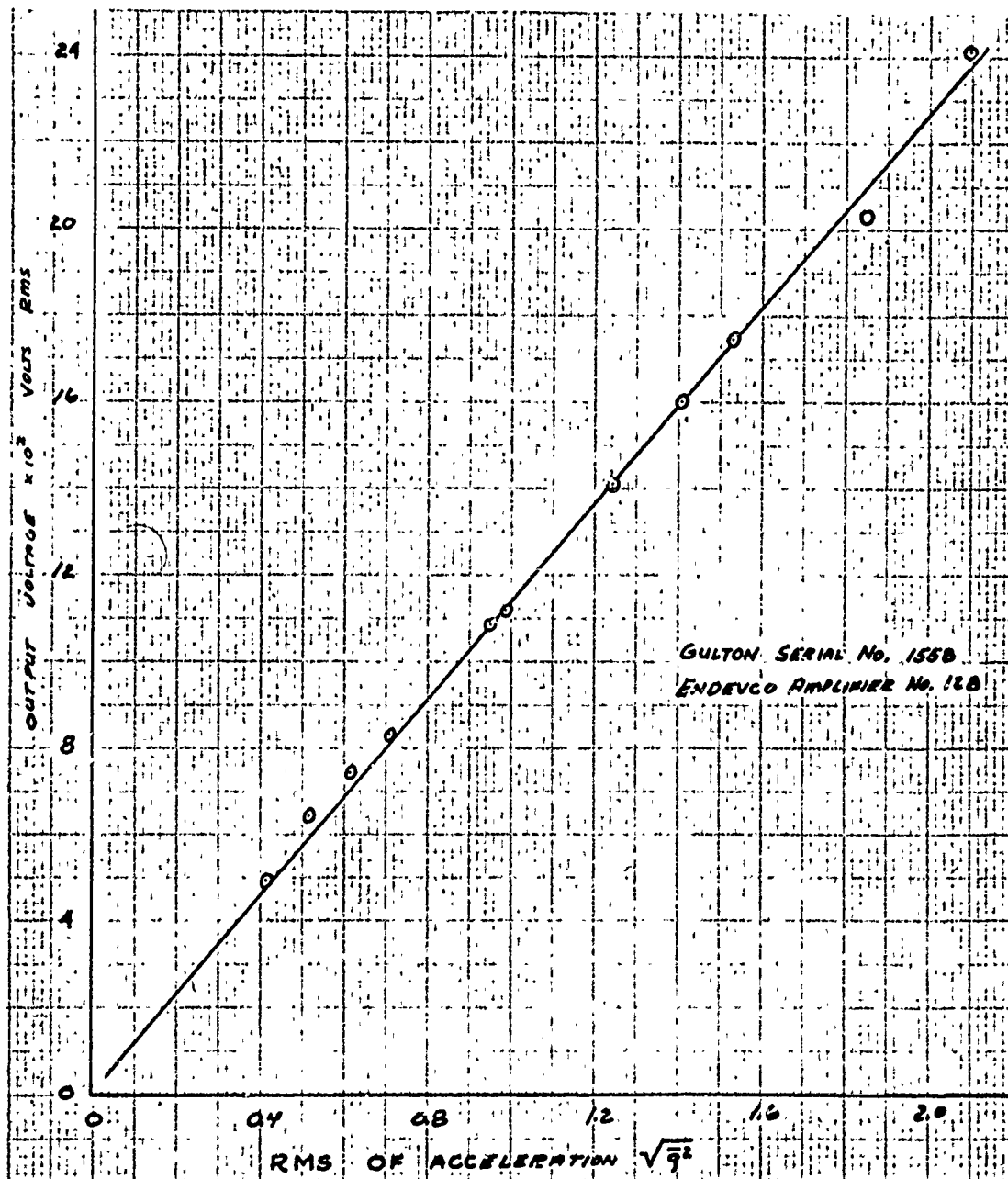


FIGURE B-2
CALIBRATION OF GULTON ACCELEROMETER



APPENDIX C

BRUSH OSCILLOGRAPH TRACES OF DATA
AND FREQUENCY RESPONSES

Typical brush recorder tracings of response data of the aeroelastic model to the random forcing function are shown on Figure C-1. The lever arm and average frequency are shown on each trace.

Typical brush recorder tracings of the static frequency response test are shown in Figure C-2. These are used to determine the system natural frequency (f_n) and damping (β).

FIGURE C-1

TYPICAL BRUSH RECORDER TRACINGS OF RESPONSE DATA

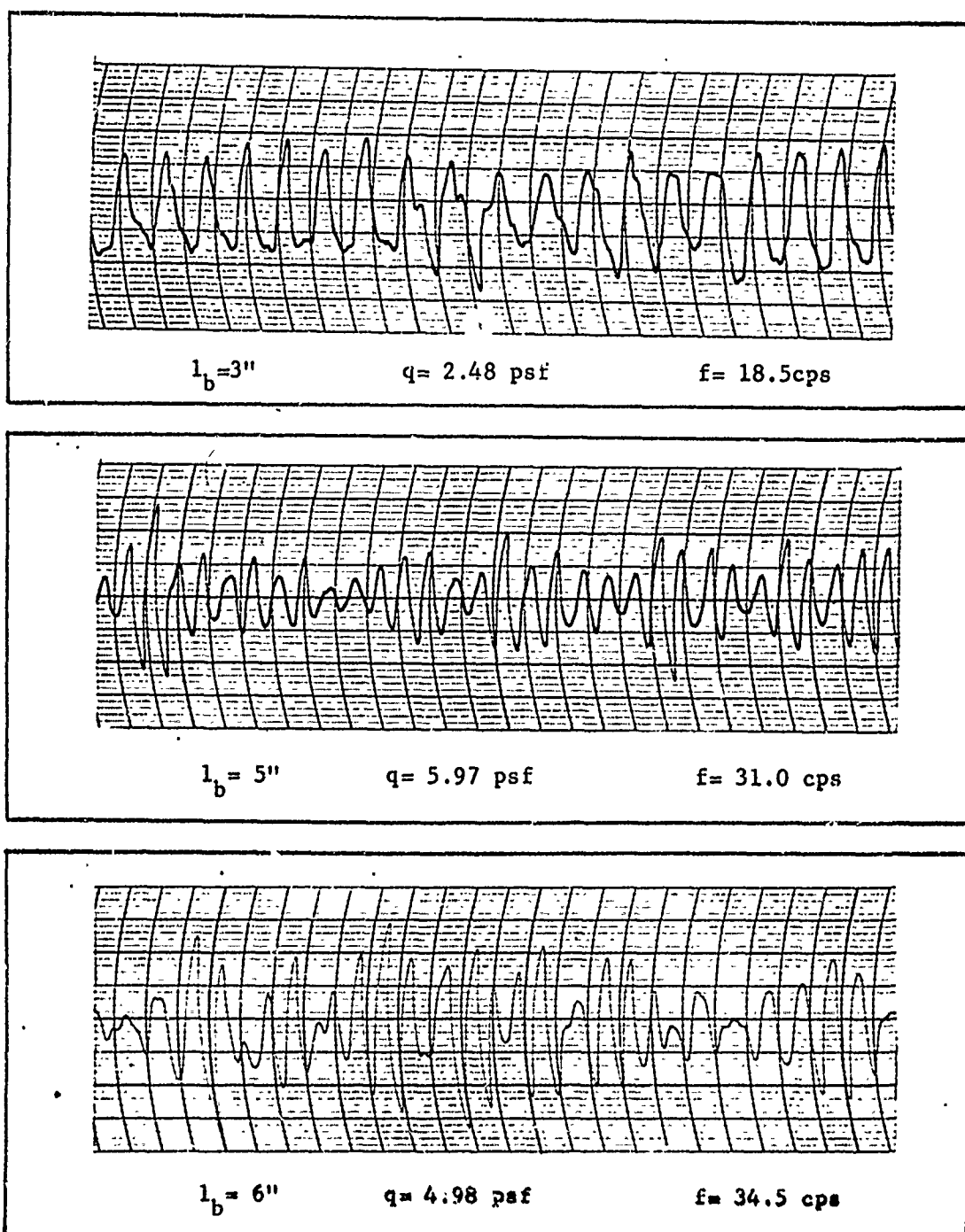
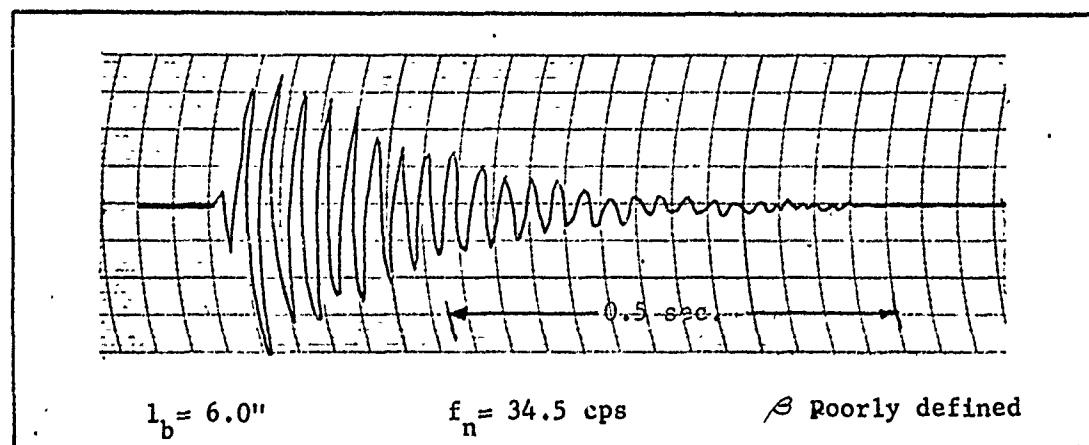
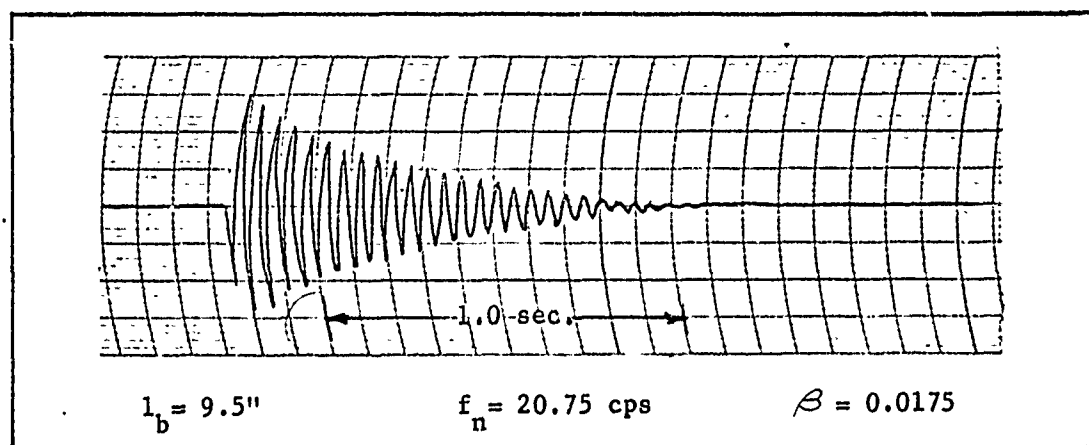


FIGURE C-2
TYPICAL BRUSH RECORDER TRACINGS OF
STATIC FREQUENCY RESPONSES.



APPENDIX D

ANALOG TO DIGITAL CONVERSION SYSTEM

The process of converting real analog data into computer digital form was accomplished by the system shown in Figure D-1. The system utilized the C.D.C. 160 computer with Program Digitize, Table D-1, to sample the analog data digitize and write the digital form on magnetic tape compatible with the C.D.C. 1604 computer. Program Test, Table D-2, is used to calibrate the system to insure accuracy. The data in digital form may be recalled by utilizing subroutine Data, Table E-2, which in turn utilizes subroutine Findit, Table E-3, which locates the pre-set identifier on the tape and subroutine Unpack, Table E-4, a machine language routine which unpacks the data. In order to test the capabilities of the digitizing system a test tape was prepared, The first 160 points of each is plotted in Figures D-2A through D-2E.

TABLE D-1
PROGRAM DIGITIZE

0	0101	PTA	
1	0603	ADN03	Jump #to
2	7064	JPI64	Initial
3	7500	EXF00	
4	2410	2410	Set enable
5	7500	EXF00	
6	1401	1401	A/D Ch. 1
7	7600	INA	
10	4176	STI76	
11	2076	LDD76	
12	3465	SBD65	
13	6134	NZF34	60 to 47
14	7500	EXF00	
15	2400	2400	Clear enable
16	2074	LDD74)	
17	4160	STI60)	
20	2067	LDD67))	Form indent
21	4161	STI61)	
22	2075	LDD75)	
23	4162	STI62)	
24	2073	LDD73)	
25	4163	STI63	
26	7500	EXF00	
27	2111	2111	163 T. V.
30	7303	OUT03	Output From
31	0000	C 0000	LWA + 1
32	6102	NZF02	
33	0133	0133	
34	2246	LDF46	0137 A
35	4076	STD76	
36	2075	LDD75	
37	3473	SBD73	
40	6155	NZF55	GØ to 0115
41	0401	LDN01	
42	4075	STD75	Set block No. = 1
43	5455	AØD55	
44	3454	SBD54	
45	6153	NZF53	GØ TØ 0120
46	6061	ZJF61	GØ TO D127
47	5476	AØD76)	
50	2066	LDD66))	Inter sample
51	0701	SBN01)	delay loop
52	6501	NZB01)	
53	7056	JPI56)	
54	0760	0760	Max blocks 760
55	0000	0000	Total block count

TABLE D-1 (Con't.)

56	0005	0005	
57	0003	0003	
60	0133	0133	1st word address
61	0134	0134	2nd of header
62	0135	0135	3rd of address
63	0136		LWA of header
64	0100		Addr of initial
65	0000	C	LWA of data
66	0000	M	Inter sample delay
67	0000	M	Spare ID (anything)
70	0000	M	Initial run no
71	0000	M	No runs wanted
72	0000	M	No samples/block
73	0000	M	No blocks/run
74	0000	C	Current run number
75	0000	C	Current block number
76	0000	C	Running Storage Address
77	0000	C	Jump control
100	4077	STD77	Enter initial
101	2200	LDC00	
102	0137	0137	
103	4076	STD76	Set FWA of data
104	3072	ADD72	Compute LWA + 1
105	4031	STD31	
106	0701	SBN01	
107	4065	STD65	Set LWA of data
110	2070	LDD70	Load initial run no.
111	4074	STD74	Set I. R. N.
112	0401	LDN01	
113	4075	STD75	Set I. B. N.
114	7077	JPI77	Exit initial
115	5475	AOD75	Update block no.
116	5455	AOD55	Update block count
117	7057	JPI57	Go to 0003
120	2074	LDD74	
121	3471	SBD71	Check no. runs enough
122	6103	NZF03	
123	2074	LDD74	Current run no.
124	7701	MLT01	
125	5474	AOD74	Update run no.
126	7057	JPI57	Go to 0003
127	7500	EXFOO	
130	1111	1111	
131	2055	LDD55	Display total block count
132	7702	HLT02	

TABLE D-1 (Con't.)

133	0000	Run no. 10
134	0000	Spare ID
135	0000	Block ID
136	0000	No. blocks/run ID
137)	
7776)) Data storage area	

Note: M = Manual entry
C = Computed entry

TABLE D-2
PROGRAM TEST-160

0	7500	EXFOO	Set enable
1	2410	2410	
2	7500	EXFOO	Call A/D CH 1
3	1401	1401	
4	7600	INA	
5	4070	STD70	
6	7500	EXFOO	
7	2401	2401	
10	7303	OUT03	Output
11	0072	0072	From 0071 to 0072
12	6102	NZF02	
13	0070	0070	
14	0400	LDN00	
15	4071	STD71	
16	6414	EJB14	Return to 000Z
17	7700	HLT00	
20	7500	EXFOO	Set enable
21	2410	2410	
22	7500	EXFOO	Call A/D CH 1
23	1401	1401	
24	7600	INA	
25	4143	STI43	
26	0300	NØP	
27	0300	NØP	
30	0300	NØP	
31	0300	NØP	
32	0300	NØP	
33	0300	NØP	
34	0300	NØP	
35	0300	NØP	
36	2042	LDD42	
37	0701	SEN01	
40	6501	NZB01	
41	7044	JPI44	
42	M	Timing control word	
43	0043	0043	
44	0022		
45	7701	HLT01	

FIGURE D-1

DIAGRAM OF ANALOG TO DIGITAL CONVERSION SYSTEM

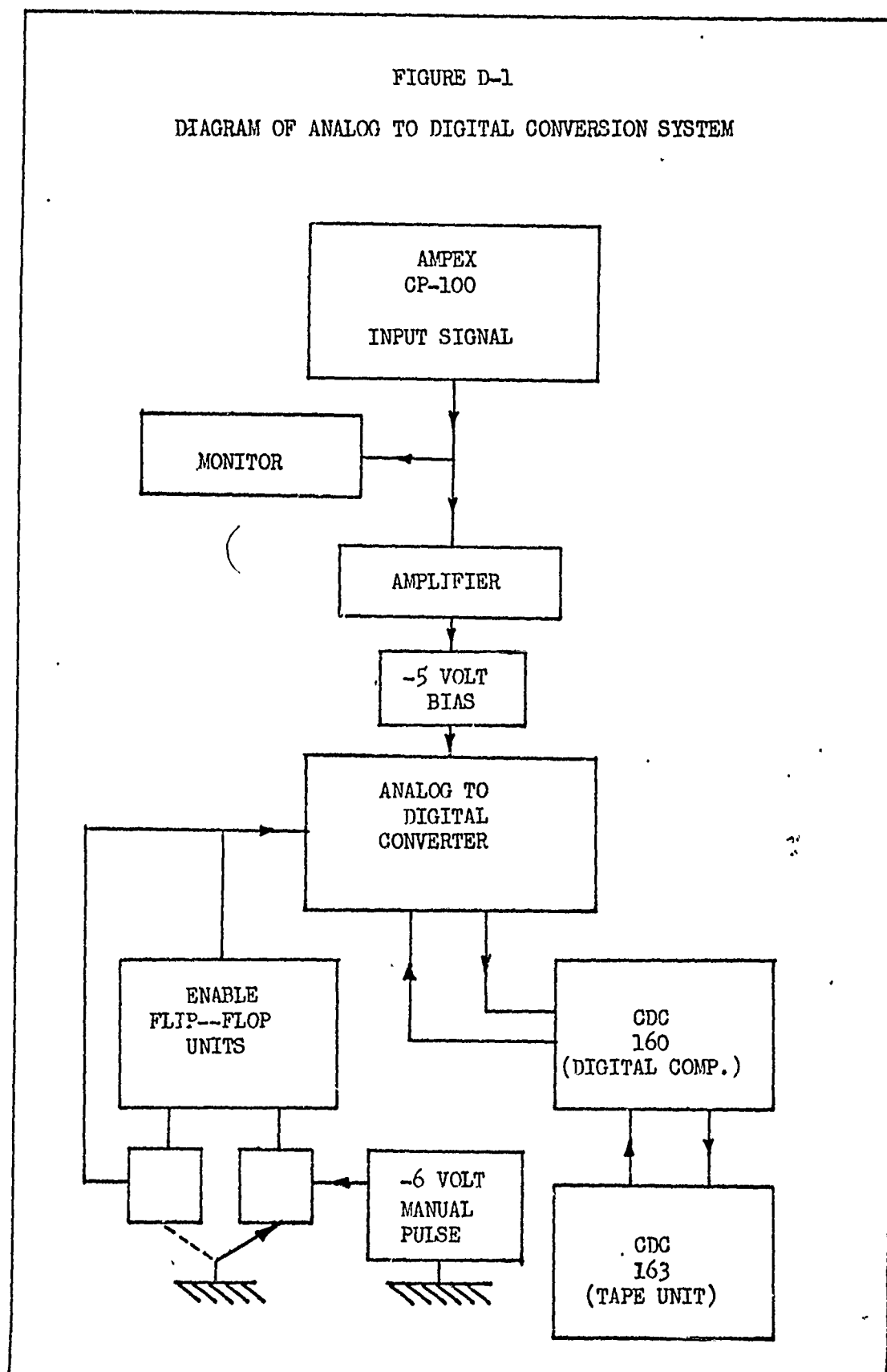
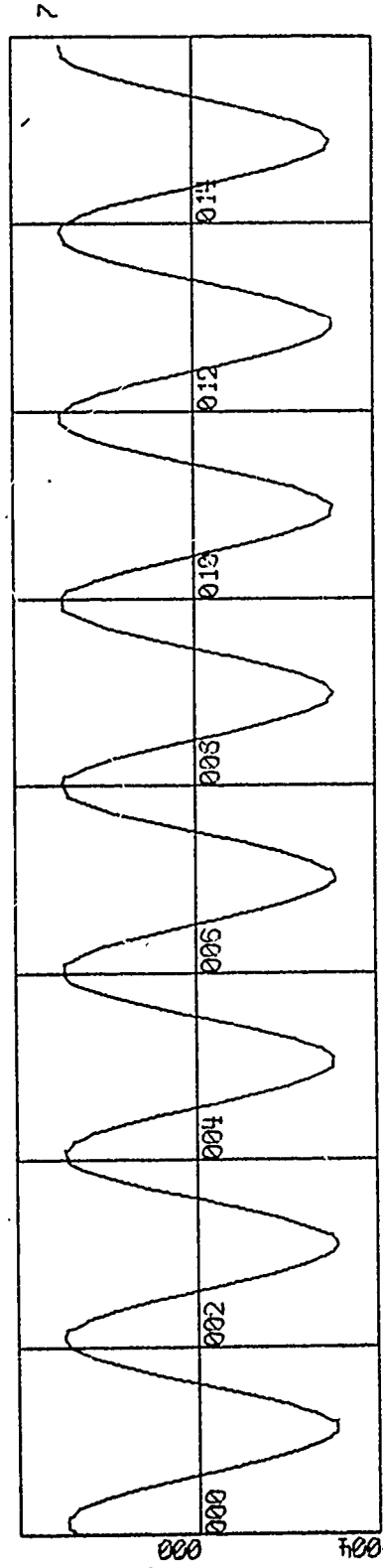


FIGURE D-2A

250 CYCLE PER SECOND SINE WAVE



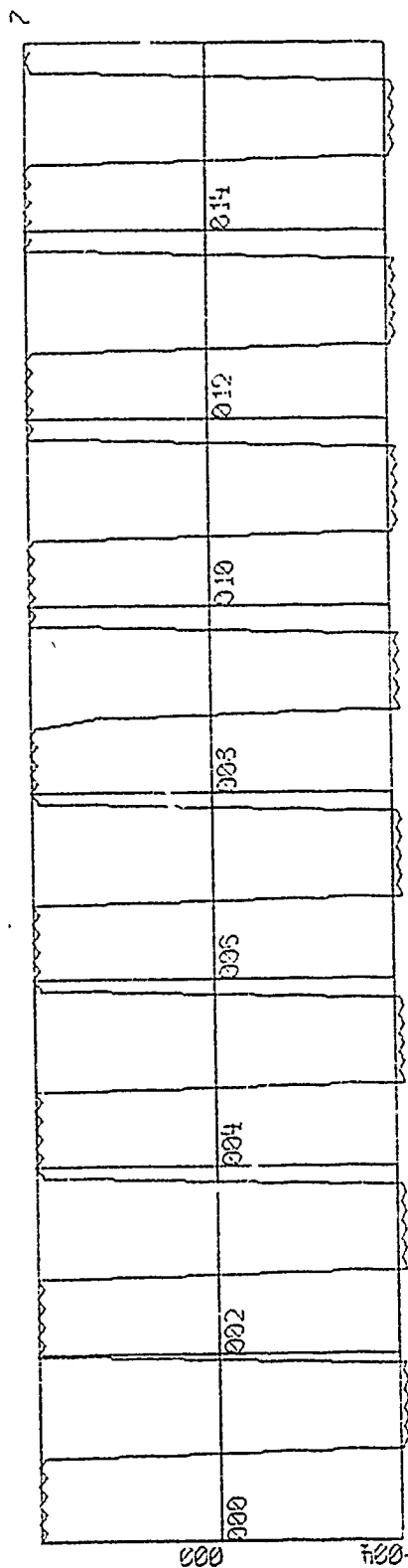
X-SCALE = $2.00E+01$ UNITS/INCH.

Y-SCALE = $4.00E+00$ UNITS/INCH.

JESBERG FIRST HUNDRED SIXTY POINTS OF INPUT DATA
FROM DIGITAL TEST TAPE

FIGURE D-2B

250 CYCLE PER SECOND SQUARE WAVE



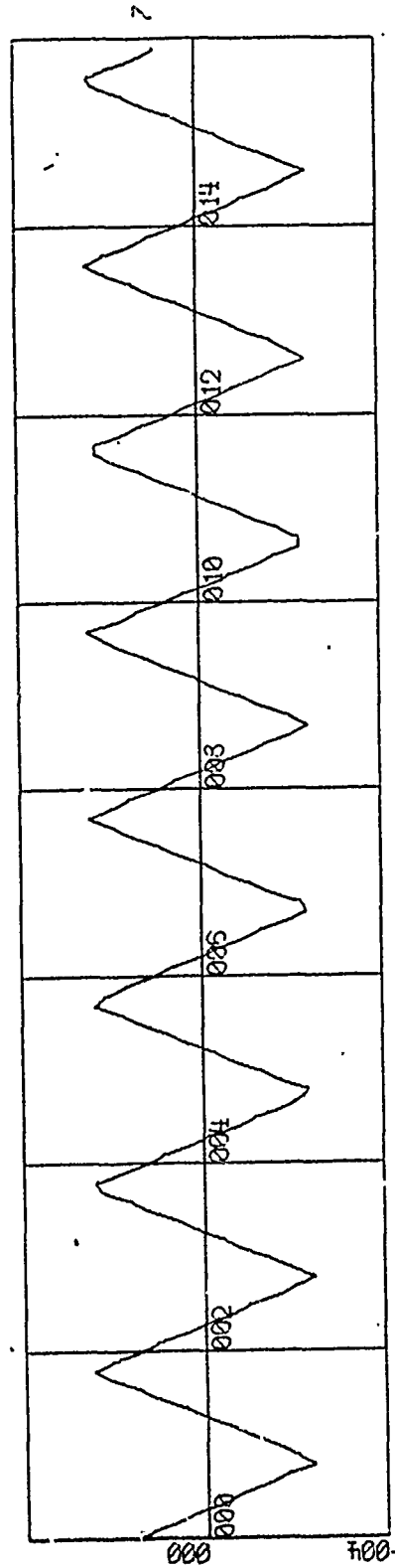
X-SCALE - 2.00E+01 UNITS/INCH.

Y-SCALE - 4.00E+00 UNITS/INCH.

JESBERG FIRST HUNDRED SIXTY POINTS OF INPUT DATA
FROM DIGITAL TEST TAPE

FIGURE D-2C

250 CYCLE PER SECOND TRIANGULAR WAVE



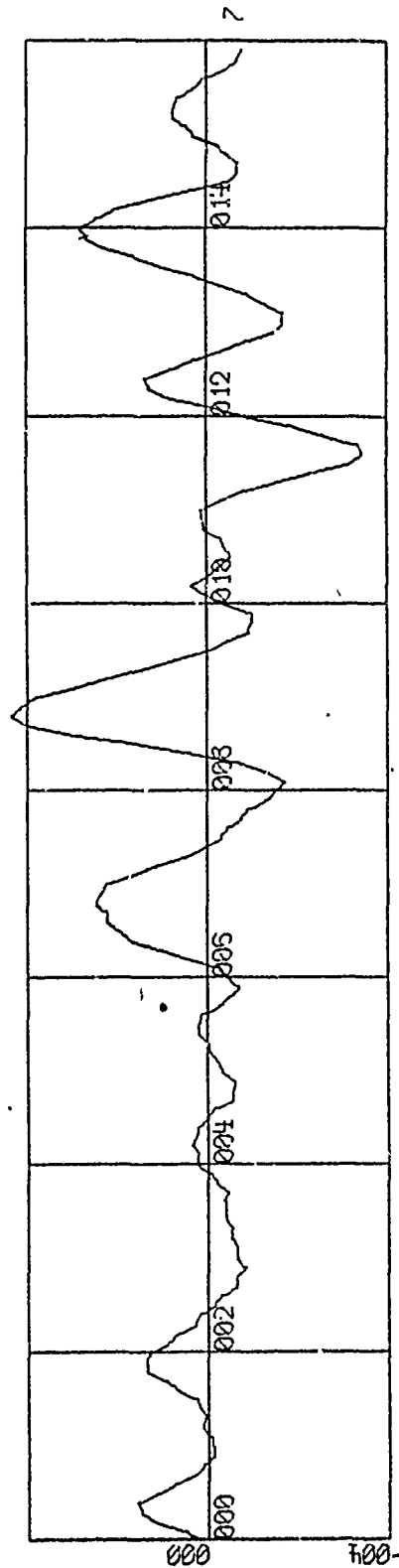
X-SCALE = $2.00E+01$ UNITS/INCH

Y-SCALE = $4.00E+00$ UNITS/INCH

JESBERG FIRST HUNDRED SIXTY POINTS OF INPUT DATA
FROM DIGITAL TEST TAPE

FIGURE D-2D

20 CYCLE PER SECOND BAND LIMITED WHITE NOISE

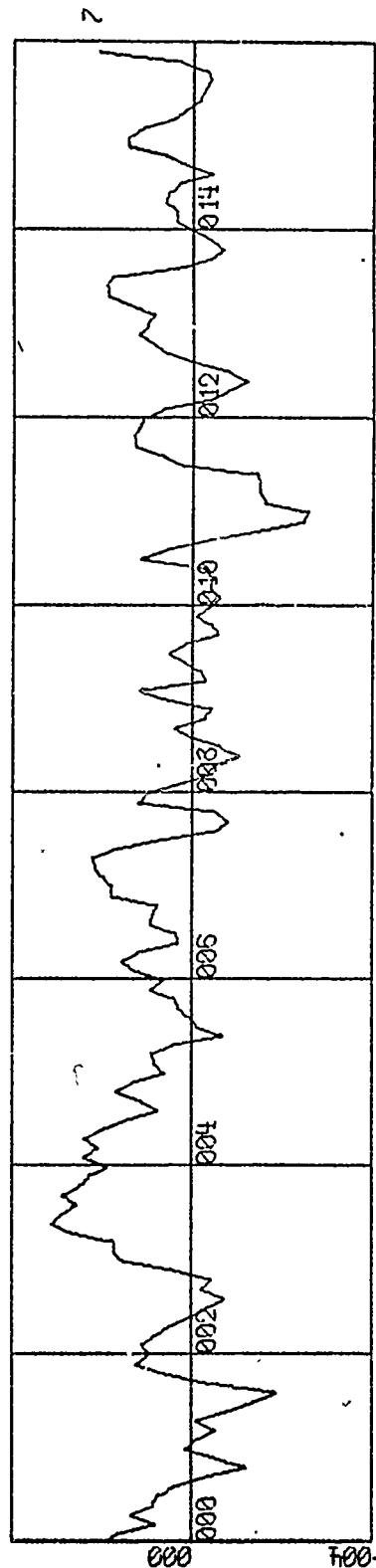


U-SCALE = 2.00E+01 UNITS/INCH.
Y-SCALE = 4.00E+00 UNITS/INCH.

JESBERG FIRST HUNDRED SIXTY POINTS OF INPUT DATA
FROM DIGITAL TEST TAPE

FIGURE D-2E

WHITE NOISE



X-SCALE = $2.00E+01$ UNITS/INCH.

Y-SCALE = $4.00E+00$ UNITS/INCH.

JESBERG FIRST HUNDRED SIXTY POINTS OF INPUT DATA
FROM DIGITAL TEST TAPE

APPENDIX E

POWER SPECTRAL DENSITY PROGRAM

The energy distribution on an average basis in the frequency domain is defined by the power spectral density. A computer program utilizing the Tukey method for estimating spectral distribution was written - Table E-1. Tables E-2 through 4 are subroutines which locate and unpack the data desired. The program has sufficient comments to make it self-explanatory. Figure E-1 is an illustration of the control card utilized in the program. A sample listing of the data output is given in Table E-5 and graphically presented in Figure E-2. The data and graphs specifically define the frequency response of the aeroelastic model to the random aerodynamic forcing function.

It will be noted in Table E-5 that the first 100 values of input data are listed in order to give visual assurance that the numbers are valid. The listing of auto-correlation is normalized with respect to its value at $\tau = 0$ and is specified as $AN(\tau)$ versus $\tau(\text{SEC})$. The value $A(0)$ shown above the listing is the actual mean square value of the auto-correlation at time shift $\tau = 0$ seconds, and is in units of $(\text{volts})^2$. This value may be related to the tape recorder voltage signal by the scaling factor of 5.0 volts (digitized) = 1.4 volts (recorded). The power spectral density is listed as $XN(\text{FREQ})$ versus $\text{FREQ}(\text{CPS})$ and is normalized such that the area under the curve of XN versus FREQ is unity.

TABLE E-1
POWER SPECTRAL DENSITY COMPUTER PROGRAM

```

-COOP,,JESBERG BOX J,I/1/0/49/S/1S/2S/E/45=54/5=50/6=51,15,20000.
-FTN,L,E.
      PROGRAM POWSPEC
C      TUKEY METHOD FOR ESTIMATING POWER SPECTRAL DENSITIES
      DIMENSION P(4000),A(501),X(501),FREQ(501),TAU(501),Q(3000)
      DIMENSION KDATA(4000,2),IDENT(200)
      DIMENSION ITITLE(12)
      DIMENSION DATE(160),SKIP(160)
      COMMON KDATA
      EQUIVALENCE (KDATA,P)
C      FIRST STEP IS DATA CONTROL CARD--DATA READ IN BY TAPE OR CARD
C      FIND IF DATA IS ON TAPE--ITAPE=0 FOR TAPE,=1 FOR CARD DATA
      WRITE (6,103)
1      READ (5,101) ITAPE,IDELTA,DELTAT,ISTART,IMAX,M
      WRITE (6,104)
      WRITE(6,101) ITAPE,IDELTA,DELTAT,ISTART,IMAX,M
      IQ=ISTART-1
      IADJ=IMAX-IQ
2      IF(ITAPE - 1) 6,5,5
C      START DATA CARD READ IN--USE THIS BRANCH FOR TEST PURPOSES
C      IF CARD DATA REMOVE STATEMENT 11 AND REPLACE WITH A CONTINUE
5      READ (5,102) (P(I),I=1,IMAX)
      WRITE (6,105)
      WRITE (6,106) (P(I),I=1,100)
      GO TO 30
C      START TAPE DATA READ IN--USE THIS BRANCH FOR PRODUCTION
C      NUMHDR = NO. OF HEADINGS
6      READ 110,NUMHDR
      DO 7 N=1,NUMHDR
7      READ 111,IDENT(N)
      WRITE (6,114)
      WRITE (6,111) (IDENT(N),N=1,NUMHDR)
C      MAIN DO LOOP ON ENTIRE PROGRAM
      DO 500 N=1,NUMHDR
      IDENT =IDENT(N)
      KLIST=1
      MAX=IMAX
      CALL DATA(IDENT,MAX,KLIST,KFLAG)
      IF(KFLAG) 8,9,8
8      WRITE (6,112)
      WRITE (6,113) N,IDENT
      GO TO 500
9      DO 11 J=1,IMAX
      I=1
10     P(J)=KDATA(J,I)
11     P(J)=P(J)/(-409.6)
      WRITE (6,105)
      WRITE (6,106) (P(I),I=1,100)
      GO TO 30

```

TABLE E-1 (Con't.)

```

C    NORMALIZE INPUT DATA TO WIPE OUT D-C TERM ON AVERAGE BASIS
30  ASUM=0.0
31  DO 32 I=1,IADJ,IDELTA
    ASUM=ASUM+P(I)
32  CONTINUE
C    AZ IS NUMBER OF DATA SAMPLES BEING COMPUTED
    AZ=FLOATF((IADJ-1)/(IDELTA))+1.0
    ASUM=(ASUM)/(AZ)
33  DO 34 I=1,IADJ,IDELTA
    P(I)=P(I)-ASUM
34  CONTINUE
    ASIS=0.0
    DO 35 I=1,160
    DATE(I)=P(I)
    SKIP(I)=ASIS
    ASIS=ASIS+1.0
35  CONTINUE
C    FIND MEAN SQUARE AZERO    I.E. AUTOCORRELATION AT TAU=ZERO
40  ASUM=0.0
41  DO 42 I=1,IADJ,IDELTA
    ASUM=ASUM+P(I)**2
42  CONTINUE
    AZERO=ASUM/AZ
C    FIND AUTO-CORRELATIONS A(L) FOR L=1,M
43  DO 46 L=1,M
    ASUM=0.0
    BSUM=0.0
    CSUM=0.0
    MZ=(L*IDELTA+1)
44  DO 45 I=MZ,IADJ,IDELTA
    IZ=I-(L*IDELTA)
    ASUM=ASUM+P(IZ)*P(I)
    BSUM=BSUM+P(IZ)
    CSUM=CSUM+P(I)
45  CONTINUE
    AZ=(1.0)/FLOATF(((IADJ-1)/(IDELTA))+1-L)
    A(L)=(AZ)*(ASUM)-(AZ**2)*BSUM*CSUM
46  CONTINUE
C    FIND XZERO---POWER SPECTRAL DENSITY AT FREQ=ZERO
50  ASUM=0.0
    MZ=M-1
    FM=FLOATF(M)
    CS1=COSF(3.14159/FM)
    SN1=SINF(3.14159/FM)
    CSL=CS1
    SNL=SN1

```

TABLE E-1 (Con't.)

```

51 DO 52 L=1,MZ
C   AZ=HANNING FACTOR
C   FIND COSINE SUM FROM TRIG. IDENTITIES
    AZ=1.0+CSL
    ASUM=ASUM+AZ*A(L)
    CSL1=CSL*CS1-SNL*SN1
    SNL1=SNL*CS1+CSL*SN1
    CSL=CSL1
    SNL=SNL1
52 CONTINUE
    DZ=0.5/FM
    XZERO=DZ*(ASUM+AZERO)
C   FIND X(K)---POWER SPECTRUM AT K=1,M
    CSK=CS1
    SNK=SN1
53 DO 59 K=1,M
    ASUM=0.0
    CSKL=CSK
    SNKL=SNK
    CSL=CS1
    SNL=SN1
54 DO 55 L=1,MZ
    AZ=(1.0+CSL)*CSKL
    ASUM=ASUM+AZ*A(L)
    CSL1=CSL*CS1-SNL*SN1
    SNL1=SNL*CS1+CSL*SN1
    CSL=CSL1
    SNL=SNL1
    CSKL1=CSKL*CSK-SNKL*SNK
    SNKL1=SNKL*CSK+CSKL*SNK
    CSKL=CSKL1
    SNKL=SNKL1
55 CONTINUE
    IF(K-M)56,57,57
56 DZ=1.0
    GO TO 58
57 DZ=0.5
    GO TO 58
58 DZ=DZ/FM
    X(K)=DZ*(ASUM+AZERO)
    CSK1=CSK*CS1-SNK*SN1
    SNK1=SNK*CS1+CSK*SN1
    CSK=CSK1
    SNK=SNK1
59 CONTINUE

```


TABLE E-1 (Con't.)

```

C      SHIFT INDICES--ZERO FREQ WILL START AT K=1 AFTER SHIFT
C      USE STORAGE SPACE OF P(I) DATA DURING SHIFT OPERATION
C      NORMALIZE AUTOCORRELATION
C      NORMALIZE AUTOCORRELATION W.R.T. AZERO
60 DO 61 I=1,M
    P(I+1)=X(I)
    P(I+1001)=A(I)
61 CONTINUE
    X(1)=XZERO
    A(1)=1.0
    MZ=M+1
62 DO 63 I=2,MZ
    X(I)=P(I)
    A(I)=P(I+1000)/(AZERO)
63 CONTINUE
C      APPLY TRAP. RULE TO FIND ENERGY CONTAINED IN POWER SPECTRUM
C      FOR RANGE OF K=1,M+1---DEFINE ENERGY AS XENGY
C      NOTE X(K) IS ENERGY (W.R.T. UNIT CHANGE OF INDEX K
    ASUM=0.0
65 DO 66 K=2,M
    ASUM=ASUM+X(K)
66 CONTINUE
    XENGY=0.5*(X(1)+2.*ASUM+X(M+1))
C      FIND FRACTION OF TOTAL ENERGY IN CALCULATED FREQ. RANGE
    XFACT=XENGY/AZERO
C      OBTAIN SPECTRAL DENSITY W.R.T. FREQ(CPS)--NORMALIZE W.R.T XENGY
    FREQ(1)=0.0
    TAU(1)=0.0
    MZ=M+1
67 DO 68 K=1,MZ
    AZ= 2.0*(DELTAT)*FM
    X(K)=(AZ)*X(K)/XENGY
    FREQ(K+1)=FREQ(K)+(1.0)/(AZ)
    TAU(K+1)=TAU(K)+DELTAT
68 CONTINUE

```

TABLE E-1 (Con't.)

C POWER SPECTRUM WRITE OUT INSTRUCTIONS

```

70 WRITE (6,103)
   WRITE (6,107) XFACT,AZERO
   WRITE (6,108)
   WRITE (6,109) (TAU(K),A(K),FREQ(K),X(K),K=1,MZ)
   LABEL=4H
   ITITLE(1)=8HJESBERG
   ITITLE(2)=8HPOWER SP
   ITITLE(3)=8HECTRAL D
   ITITLE(4)=8HENSITIES
   ITITLE(5)=8H -- RUN
   READ (5,115) ITITLE(6)
   DO 80 J=7,12
80  ITITLE(J)=8H
   CALL DRAW(125,FREQ,X,0,0,LABEL,ITITLE,20,,2,0,0,2,2,8,2,1,LAST)
500 CONTINUE
101 FORMAT (2I2,F8.5,2I6,I3)
102 FORMAT(12F6.4)
103 FORMAT (99H1 T U K E Y   S P E C T R U M   E S T I M A T E S .
104          1POWER SPECTRAL DENSTIY AND AUTO-CORR. CALCS.      //)
104 FORMAT (20H DATA CONTROL CARD //)
105 FORMAT (30H0 DATA RECORD--(P(1)=1,100)      //)
106 FORMAT (10F8.3)
107 FORMAT (8H XFACT= F8.5,8H A(0)= F12.5 //)
108 FORMAT (42H TAU(SEC) AN(TAU) FREQ(CPS) XN(FREQ) //)
109 FORMAT (F9.3,F10.5,F12.3,F10.5)
110 FORMAT(3X,I4)
111 FORMAT (3X,016)
112 FORMAT(31H1 ERROR IN SR DATA AT HEADING )
113 FORMAT(40X,I3,7X,016)
114 FORMAT (22H IDENT(N),N=1,NUMHDR //)
115 FORMAT(3XA8)
END

```

TABLE E-2

```

SUBROUTINE DATA(IDENT,MAX,KLIST,KFLAG)
DIMENSION IBLOCK(1001),KDATA(4000,2)
COMMON KDATA, IBLOCK
CALLING INSTRUCTIONS FOR SUBROUTINE DATA
C   ARG 1. IDENT IS A 16 OCTAL DIGIT IDENTIFYING NUMBER
C   SUPPLIED BY THE 160 PROGRAM WHEN TAPE WAS MADE.
C   THE CALLING PROGRAM MUST SUPPLY THIS NUMBER IN ORDER FOR
C   THE CORRECT BLOCK OF DATA TO BE RECALLED.
C   ARG 2. MAX IS THE NUMBER OF SAMPLES PER BLOCK AND MUST BE LESS
C   THAN 4000 DEC.
C   ARG 3. KLIST IS EITHER 1 OR 2 AND DECIDES WHICH SIDE OF
C   KDATA YOU WANT THE DATA TO BE UNPACKED INTO
C   ARG 4. KFLAG IS AN ERROR FLAG RAISED BY DATA. IF =0, NO ERROR
C   LOGICAL UNIT 1 IS USED BY DATA TO FIND BLOCK.
C   EACH TIME DATA IS CALLED IT FINDS THE DESIRED BLOCK ON THE TAPE
C   AND UNPACKS IT INTO EITHER KDATA(M,1) OR KDATA(M,2)
C   IN THE CALLING PROGRAM DIMENSION KDATA(4000,2), AND
C   DECLARE KDATA COMMON.
C   KDATA IS THE OUTPUT LIST AND IS REFERENCED BY KLIST
C   SUBROUTINE DATA CALLS ON SR UNPACK AND SR FINDIT
C   AFTER UNPACK THERE EXISTS ONE 1604 WORD/160 WORD
C   ASSIGNMENT NOS USED IN DATA,822,823,824,825,828,829
824 FORMAT(48H1 ERROR OCCURRED IN FINDIT SUBROUTINE AT HEADER )
825 FORMAT(50X,016)
828 FORMAT(33H0 I HAVE UNPACKED DATA HEADED BY ,016 )
830 FORMAT( 1X,I4, 3X,016)
CALL FINDIT(IDENT,MAX,IFLAG)
IF(IFLAG) 822,823,822
822 PRINT 824 $ PRINT 825,IDENT $KFLAG=1$ GO TO 829
823 JMAX=MAX/4+1
CALL UNPACK (IBLOCK,JMAX,KLIST,KDATA(1,KLIST))
KFLAG = 0 $ PRINT 828 , IDENT
DO 826 M=1,4
826 PRINT 830,M,KDATA(M,KLIST)
J = MAX - 3
DO 827 M = J, MAX
827 PRINT 830,M,KDATA(M,KLIST)
829 CONTINUE
END

```

TABLE E-3

```

SUBROUTINE FINDIT(IDENT,MAX,IFLAG)
DIMENSION KDATA(4000,2),IBLOCK(1001)
COMMON KDATA,IBLOCK
814 FORMAT(53H1 A PARITY ERROR WAS DETECTED BUT RUN WAS NOT STOPPED)
815 FORMAT(45H PARITY ERROR OCCURRED AT HEADER AS FOLLOWS )
816 FORMAT(33X,016)
818 FORMAT(32H1 I HAVE LOCATED DATA HEADED BY ,016 )
820 FORMAT (38H UNABLE TO LOCATE HEADING AS FOLLOWS )
      MAX1=MAX/4 + 1
      ASSIGN 811 TO JUMP
805 BUFFER IN (1,1)(IBLOCK(1),IBLOCK(MAX1))
806 IF(UNIT,1) 806,807,808,810
807 IF(IDENT-IBLOCK(1))805,813,805
808 GO TO JUMP,(811,812)
811 REWIND 1$ ASSIGN 812 TO JUMP $ GO TO 805
810 IPAR=1 $ GO TO 807
812 REWIND 1$ GO TO 819
809 PRINT 814$ PRINT 815$ PRINT 816,IDEN$ GO TO 817
813 IF(IPAR) 809,817,809
817 IFLAG = 0 $ PRINT 818,IDENT $ GO TO 821
819 PRINT 820
      PRINT 816,IDENT
      IFLAG=1
C      ASSIGNMENT NOS USED HERE,805,807,808,809,810,811,812,813,814,815
C      816,817,818,819,820,821
821 CONTINUE
      END

```

TABLE E-4
SUBROUTINE UNPACK

	IDENT	UNPACK	ARGS
UNPACK	ENTRY	UNPACK	IBLOCK,JMAX,KLIST,KDATA SUBR UNPACK CALLED BY SR DATA
	SLJ	**	+
	SIU	1 EXIT	
	LIU	1 UNPACK	+ JMAX=MAX/4+1, MOST=JMAX-1
	LDA	1 0	GETS ADDR OF CALLING ARGS
	SAL	U1	+U1 IS JMAX ADDR
	ARS	24	IBLOCK PACKED IN DATA 1001 WDS
	INA	-1	+
U1	SAU	AADRS	ADRS OF IBLOCK IN AADRS
	LDA	**	+FILLED IN BY 3 INSTRUCTIONS BACK
	SAU	BADRS	STORE JMAX IN LOOP COUNT
	LDA	1 1	+GO GET ADRS OF NEXT ARG
	SAU	J4	+STORE ADRS OF KDATA(1,KLIST)
	INA	1	ADVANCE ADRS
	SAL	J3	+STORE ADRS OF KDATA(2,KLIST)
	INA	1	
	SAU	J2	+DITTO FOR KDATA(3,KLIST)
	INA	1	
	SAL	J1	+DITTO FOR KDATA(4,KLIST)
	INI	1 2	SET CORRECT EXIT ADRS
	SIU	1 EXIT+1	+STORE IN EXIT INST
	SIL	2 EXIT	SAVE INDEX 2
	ENI	1 2	+FIRST DATA WORD IN IBLOCK
	ENI	2 0	FIRST WORD IN KDATA IS DATA
AADRS	LDA	1 **	+IBLOCK(J)
	LRS	12	SHIFT 4TH WORD INTO A REG
J1	QRS	36	+RIGHT JUST,SIGN EXTEND
	STQ	2 **	STORE IN KDATA (I+4,KLIST)
	LRS	12	+SHIFT 3RD WORD INTO Q
	QRS	36	RIGHT JUST ,SIGN EXTEND
J2	STQ	2 **	+STORE IN KDATA(I+3,KLIST)
	LRS	12	SHIFT 2ND WORD INTO A REG
J3	QRS	36	+ RIGHT JUST, SIGN EXTEND
	STQ	2 **	STORE IN KDATA(I+2,KLIST)
J4	STA	2 **	+1ST WORD NOW RT.JUST +SIGN EXT.
	INI	2 4	I=I+4
BADRS	ISK	1 **	+ISK ON JMAX
	SLJ	AADRS	J=J+1 REPEAT LOOP
EXIT	ENI	1 **	+RESTORE INDEX 1
	ENI	2 **	RESTORE INDEX 2
	SLJ	**	+ JUMP OUT

TABLE E-4 (Con't.)

	IDENT	ENTRY	UNPACK	UNPACK	ARGS IBLOCK,JMAX,KLIST,KDATA SUBR UNPACK CALLED BY SR DATA +
UNPACK	SLJ		**		
	SIU	1	EXIT		
	LIU	1	UNPACK		+ JMAX=MAX/4+1, MOST=JMAX-1
	LDA	1	0		GETS ADDR OF CALLING ARGS
	SAL		U1		+U1 IS JMAX ADDR
	ARS		24		IBLOCK PACKED IN DATA 1001 WDS
	INA		-1		+
U1	SAU		AADRS		ADRS OF IBLOCK IN AADRS
	LDA		**		+FILLED IN BY 3 INSRUCTIONS BACK
	SAU		BADRS		STORE JMAX IN LOOP COUNT
	LDA	1	1		+GO GET ADRS OF NEXT ARG
	SAU		J4		+STORE ADRS OF KDATA(1,KLIST)
	INA		1		ADVANCE ADRS
	SAL		J3		+STORE ADRS OF KDATA(2,KLIST)
	INA		1		
	SAU		J2		+DITTO FOR KDATA(3,KLIST)
	INA		1		
	SAL		J1		+DITTO FOR KDATA(4,KLIST)
	INI	1	2		SET CORRECT EXIT ADRS
	SIU	1	EXIT+1		+STORE IN EXIT INST
	SIL	2	EXIT		SAVE INDEX 2
	ENI	1	2		+FIRST DATA WORD IN IBLOCK
	ENI	2	0		FIRST WORD IN KDATA IS DATA
AADRS	LDA	1	**		+IBLOCK(J)
	LRS		12		SHIFT 4TH WORD INTO A REG
J1	QRS		36		+RIGHT JUST,SIGN EXTEND
	STQ	2	**		STORE IN KDATA (I+4,KLIST)
	LRS		12		+SHIFT 3RD WORD INTO Q
	QRS		36		RIGHT JUST ,SIGN EXTEND
J2	STQ	2	**		+STORE IN KDATA(I+3,KLIST)
	LRS		12		SHIFT 2ND WORD INTO A REG
J3	QRS		36		+ RIGHT JUST, SIGN EXTEND
	STQ	2	**		STORE IN KDATA(I+2,KLIST)
J4	STA	2	**		+1ST WORD NOW RT.JUST +SIGN EXT
	INI	2	4		I=I+4
BADRS	ISK	1	**		+ISK ON JMAX
	SLJ		AADRS		J=J+1 REPEAT LOOP
EXIT	ENI	1	**		+RESTORE INDEX 1
	ENI	2	**		RESTORE INDEX 2
	SLJ		**		+ JUMP OUT
	END				
	FINIS				
-EXECUTE.					

TABLE E-5 (Con't.)

TUKEY SPECTRUM ESTIMATES,

XFACT= .99626 A(0)= .79463

TAU(SEC)	AN(TAU)	FREQ(CPS)	XN(FREQ)
0	1.00000	C	.00749
.004	.46700	1.000	.01458
.008	-.36148	2.000	.01270
.012	-.48622	3.000	.01061
.016	.00744	4.000	.00873
.020	.41011	5.000	.00686
.024	.28462	6.000	.00610
.028	-.15434	7.000	.00614
.032	-.25875	8.000	.00617
.036	.10725	9.000	.00585
.040	.32453	10.000	.00691
.044	.07270	11.000	.00722
.048	-.24842	12.000	.00484
.052	-.21818	13.000	.00309
.056	.13418	14.000	.00344
.060	.37584	15.000	.00544
.064	.13704	16.000	.00642
.068	-.26967	17.000	.00494
.072	-.26584	18.000	.00499
.076	.08314	19.000	.00670
.080	.27917	20.000	.00655
.084	.12765	21.000	.00568
.088	-.16504	22.000	.00596
.092	-.21833	23.000	.00661
.096	.07653	24.000	.00638
.100	.28530	25.000	.00557
.104	.08008	26.000	.00494
.108	-.19886	27.000	.00591
.112	-.15890	28.000	.00934
.116	.09799	29.000	.01015
.120	.23746	30.000	.01056
.124	.06567	31.000	.01557
.128	.21386	32.000	.01536
.132	-.17481	33.000	.01345
.136	.12947	34.000	.02101
.140	.22078	35.000	.02561
.144	.00913	36.000	.02141
.148	-.17675	37.000	.01787
.152	-.14032	38.000	.01846
.156	.06086	39.000	.01716
.160	.17405	40.000	.01409
.164	.01655	41.000	.01360
.168	-.16435	42.000	.01429
.172	-.07287	43.000	.01487
.176	.11040	44.000	.01399
.180	.12215	45.000	.01616
.184	-.00197	46.000	.02042
.188	-.12345	47.000	.02651
.192	-.09501	48.000	.04243
.196	.09308	49.000	.07895
.200	.16188	50.000	.11559
.204	-.00033	51.000	.09713
.208	-.12095	52.000	.04315
.212	-.06221	53.000	.01450
.216	.04386	54.000	.00687
.220	.08959	55.000	.00322
.224	.01118	56.000	.00390
.228	-.11718	57.000	.00677
.232	-.07646	58.000	.00809

TABLE E-5 (Con't.)

.236	.07577	59.000	.00541
.240	.07764	60.000	.00286
.244	-.04312	61.000	.00214
.248	-.09855	62.000	.00167
.252	-.03908	63.000	.00147
.256	.10244	64.000	.00157
.260	.15790	65.000	.00228
.264	-.00012	66.000	.00275
.268	-.14379	67.000	.00205
.272	-.06071	68.000	.00203
.276	.06367	69.000	.00241
.280	.06875	70.000	.00190
.284	.01631	71.000	.00147
.288	-.04142	72.000	.00139
.292	-.03549	73.000	.00150
.296	.04868	74.000	.00164
.300	.03850	75.000	.00154
.304	-.07314	76.000	.00127
.308	-.07468	77.000	.00141
.312	.02519	78.000	.00090
.316	.07875	79.000	.00323
.320	.07094	80.000	.00973
.324	-.00860	81.000	.00816
.328	-.10054	82.000	.00151
.332	-.05049	83.000	.00019
.336	.04195	84.000	.00035
.340	.01117	85.000	.00019
.344	-.03365	86.000	.00021
.348	-.00610	87.000	.00012
.352	.01210	88.000	.00009
.356	.03291	89.000	.00010
.360	.03611	90.000	.00011
.364	-.04689	91.000	.00007
.368	-.07897	92.000	.00006
.372	.02279	93.000	.00007
.376	.07550	94.000	.00007
.380	.02770	95.000	.00007
.384	-.01348	96.000	.00011
.388	-.03263	97.000	.00011
.392	-.00793	98.000	.00011
.396	.04644	99.000	.00010
.400	-.00260	100.000	.00008
.404	-.09032	101.000	.00008
.408	-.04338	102.000	.00009
.412	.04343	103.000	.00008
.416	.04392	104.000	.00006
.420	.01335	105.000	.00007
.424	-.04006	106.000	.00006
.428	-.08647	107.000	.00007
.432	-.02018	108.000	.00008
.436	.05841	109.000	.00009
.440	.02209	110.000	.00008
.444	-.01934	111.000	.00008
.448	-.01749	112.000	.00008
.452	-.03598	113.000	.00008
.456	-.02005	114.000	.00009
.460	.02421	115.000	.00009
.464	.01484	116.000	.00009
.468	.00895	117.000	.00011
.472	.02298	118.000	.00012
.476	-.02714	119.000	.00008
.480	-.06413	120.000	.00011
.484	-.01527	121.000	.00014
.488	.02664	122.000	.00009
.492	.03797	123.000	.00006
.496	.03311	124.000	.00004
.500	-.03639	125.000	.00001

GRAPH TITLED
JESBERG POWER SPECTRAL DENSITIES -- RUN 64/15
HAS BEEN PLOTTED.

FIGURE E-1

CONTROL CARD FOR COMPUTER PROGRAM

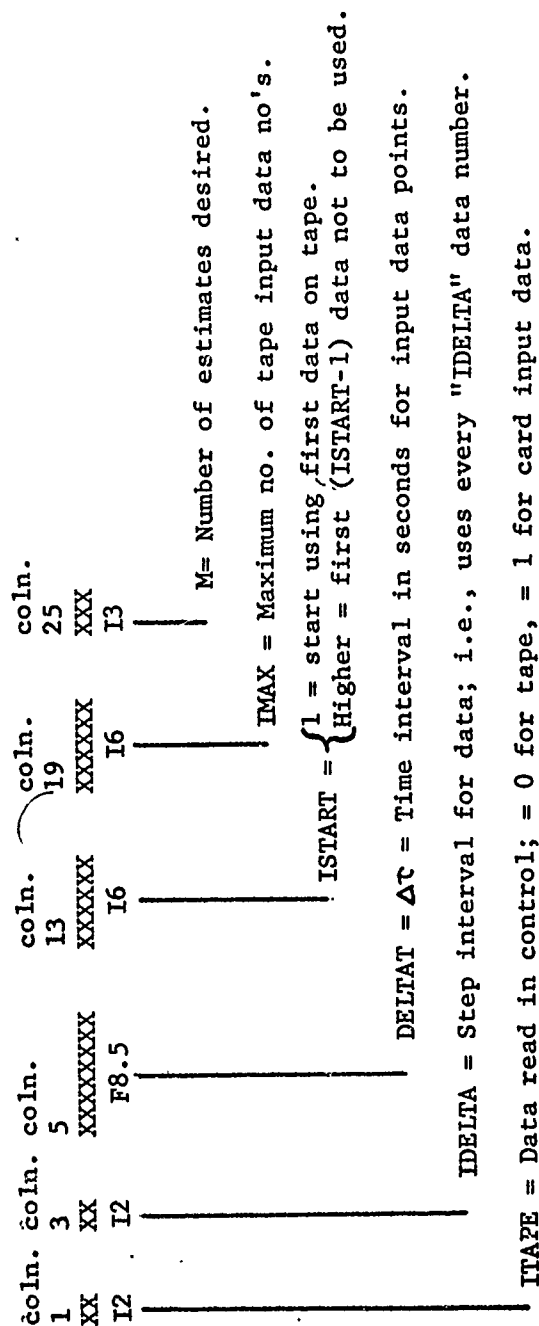
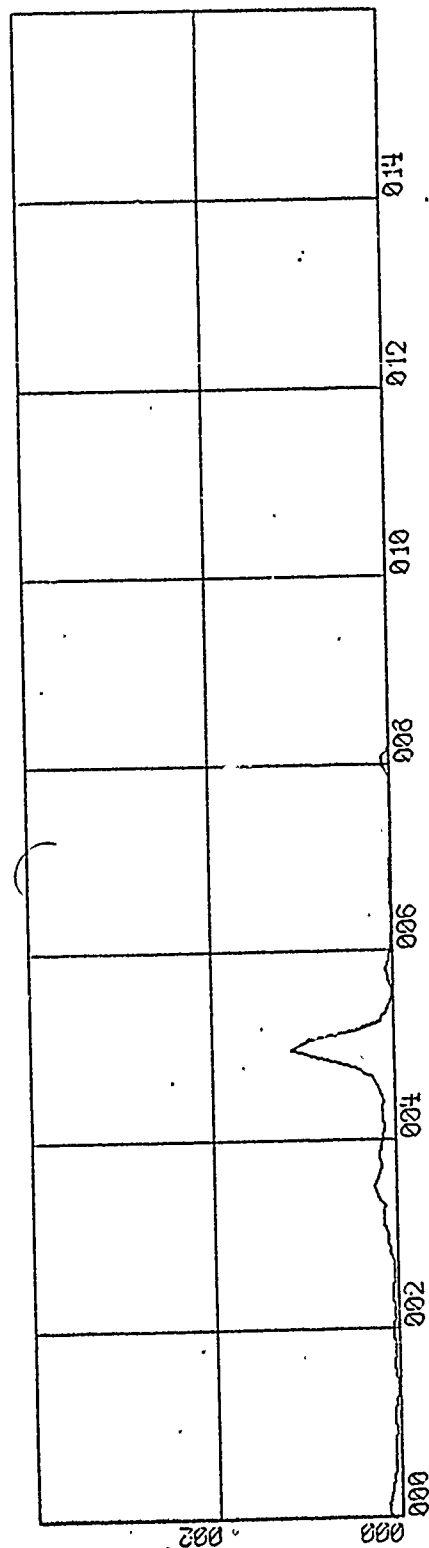


FIGURE E-2
SAMPLE GRAPHIC OUTPUT OF POWER SPECTRAL DENSITY PROGRAM



X-SCALE = 2.00E+01 UNITS/INCH.

Y-SCALE = 2.00E-01 UNITS/INCH.

JESBERG POWER SPECTRAL DENSITIES -- RUN 64/15

APPENDIX F

DEFINITION OF AUTO-CORRELATION FUNCTION AND POWER SPECTRAL DENSITY

It is well known that under certain conditions a periodic function of a real variable can be represented by a Fourier series:

$$f(t) = \sum_{n=-\infty}^{\infty} \left(a_n \cos \frac{2\pi n t}{T} + b_n \sin \frac{2\pi n t}{T} \right)$$

where T is the period of the signal and the coefficients are given by:

$$a_n = \frac{1}{2T} \int_{-T}^T f(t) \cos \frac{2\pi n t}{T} dt ; \quad b_n = \frac{1}{2T} \int_{-T}^T f(t) \sin \frac{2\pi n t}{T} dt$$

It follows from this that the power in a single periodic signal exists only at the frequency n/T cycles per second where n is any integer. The amplitude of the sinusoidal component of frequency n/T is $a_n^2 + b_n^2$. Thus the power in this component is $(a_n^2 + b_n^2)/2$. To express the power spectrum directly as a function of frequency, it is convenient to employ the Dirac delta function

$\delta(\omega - \omega_0)$ which has the following formal properties:

$$\delta(\omega - \omega_0) = 0 \quad \text{For } \omega \neq \omega_0$$

$$\int_{-\infty}^{\infty} \delta(\omega - \omega_0) f(\omega) d\omega = f(\omega_0)$$

then the power spectrum can be expressed as:

$$\phi(\omega) = \sum_{n=-\infty}^{\infty} \frac{(a_n^2 + b_n^2)}{2} \delta\left(\omega - \frac{2\pi n}{T}\right) \quad (1)$$

The auto-correlation function of a periodic function is defined as:

$$R(\tau) = \frac{1}{T} \int_{-\frac{T}{2}}^{\frac{T}{2}} f(t) f(t+\tau) dt$$

Computation of this quantity involves multiplication of the function by its time-shifted replica followed by integration over one period. Using the Fourier representation of equation (1) the correlation function of the periodic function $f(t)$ is:

$$\begin{aligned}
 R(\tau) &= \frac{1}{T} \int_{-T/2}^{T/2} \sum_{n=-\infty}^{\infty} \sum_{m=-\infty}^{\infty} \left[a_n \cos \frac{2\pi n t}{T} + b_n \sin \frac{2\pi n t}{T} \right] \\
 &\quad \left[a_m \cos \frac{2\pi m (t+\tau)}{T} + b_m \sin \frac{2\pi m (t+\tau)}{T} \right] dt \\
 R(\tau) &= \frac{1}{T} \sum_{n=-\infty}^{\infty} \int_{-T/2}^{T/2} \frac{a_n^2 + b_n^2}{2} \cos \frac{2\pi n \tau}{T} dt \\
 R(\tau) &= \sum_{n=-\infty}^{\infty} \frac{a_n^2 + b_n^2}{2} \cos \frac{2\pi n \tau}{T} \quad (2)
 \end{aligned}$$

The Fourier transform of a cosine is given by:

$$\mathcal{F}(\cos \omega_0 t) = \int_{-\infty}^{\infty} \cos \omega_0 t e^{-i\omega t} dt = \delta(\omega - \omega_0) \quad (3)$$

thus, it is readily seen from equations 1, 2 and 3 that for a periodic function

$$\begin{aligned}
 \phi(\omega) &= \int_{-\infty}^{\infty} R(\tau) e^{-i\omega \tau} d\tau \\
 R(\tau) &= \frac{1}{2\pi} \int_{-\infty}^{\infty} \phi(\omega) e^{i\omega \tau} d\omega
 \end{aligned}$$

that is, the power spectrum and auto-correlation function of a periodic signal constitute a transform pair. The equations are known as the Wiener-Khintchine relations. By letting $\tau=0$ we obtain directly the Parseval theorem

$$\frac{1}{T} \int_{-T/2}^{T/2} f^2(t) dt = R(0) = \frac{1}{2\pi} \int_{-\infty}^{\infty} \phi(\omega) d\omega$$

This relation states that the power in a periodic signal can be obtained either by averaging the square of the signal over one period or by integrating the power spectrum [3].

The definition of the auto-correlation function and power spectral density are quite clear for a periodic signal. However, a stationary random function is considered in this report.

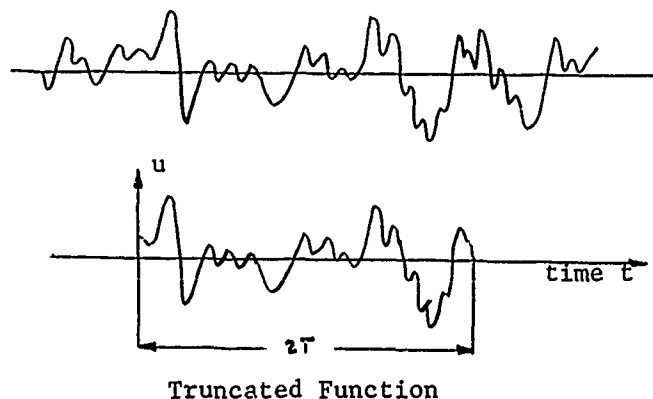
Let $u(t)$ represent a random function of time. Normally a complete statistical description is necessary to define a random signal. For dynamic-load problems in aeroelasticity a time average concept may be used. The mean and the mean square of a function of time $u(t)$ over a time interval $2T$ are:

$$\overline{u(t)} = \frac{1}{2T} \int_{t_0-T}^{t_0+T} u(t) dt$$

$$\overline{u^2(t)} = \frac{1}{2T} \int_{t_0-T}^{t_0+T} u^2(t) dt$$

If the time average is independent of t_0 and T when T is sufficiently large, then $u(t)$ is said to be stationary.

Assume that the function $u(t)$ is observed for a long period $2T$, and that it vanishes outside the interval $2T$. Further assume that $2T$ is greater than any characteristic time of the random function. Hence $u_T(t)$ represents all average statistical properties of the random function.



Since the truncation process assures absolute convergence and no finite discontinuities exist, the Fourier transform and inverse exist. Therefore,

$$\begin{aligned}\mathcal{F}_T(\omega) &= \frac{1}{\sqrt{2\pi}} \int_{-T}^T u_T(t) e^{-i\omega t} dt \\ u_T(t) &= \frac{1}{\sqrt{2\pi}} \int_{-\infty}^{\infty} \mathcal{F}_T(\omega) e^{i\omega t} d\omega\end{aligned}\quad (4)$$

since $u(t)$ is real

$$\mathcal{F}_T(\omega) = \mathcal{F}_T^*(-\omega) \quad (5)$$

where \mathcal{F}^* is the complex conjugate.

The auto-correlation function is defined as:

$$R(\tau) = \overline{u(t) u(t+\tau)} = \lim_{T \rightarrow \infty} \frac{1}{2T} \int_{-T}^T u(t) u(t+\tau) dt \quad (6)$$

substituting the transform definition of $u(t+\tau)$

$$R(\tau) = \lim_{T \rightarrow \infty} \frac{1}{2T} \int_{-T}^T u(t) \left\{ \frac{1}{\sqrt{2\pi}} \int_{-\infty}^{\infty} \mathcal{F}_T(\omega) e^{i\omega(t+\tau)} d\omega \right\} dt$$

rearranging the order of terms,

$$\begin{aligned}R(\tau) &= \lim_{T \rightarrow \infty} \frac{1}{2T} \int_{-\infty}^{\infty} \mathcal{F}_T(\omega) e^{i\omega\tau} \left\{ \frac{1}{\sqrt{2\pi}} \int_{-T}^T u_T(t) e^{i\omega t} dt \right\} d\omega \\ \mathcal{F}_T^*(\omega) &= \mathcal{F}_T(-\omega) = \frac{1}{\sqrt{2\pi}} \int_{-T}^T u_T(t) e^{-i\omega t} dt\end{aligned}$$

finally:

$$R(\tau) = \lim_{T \rightarrow \infty} \frac{1}{2T} \int_{-\infty}^{\infty} \mathcal{F}_T(\omega) \mathcal{F}_T^*(\omega) e^{i\omega\tau} d\omega$$

define:

$$\phi(\omega) = \lim_{T \rightarrow \infty} \frac{1}{T} \left| \mathcal{F}_T(\omega) \right|^2 \quad (7)$$

$$R(\tau) = \frac{1}{2} \int_{-\infty}^{\infty} \phi(\omega) e^{i\omega\tau} d\omega$$

since by setting $\tau=0$

$$R(0) = \overline{u^2(t)} = \frac{1}{2} \int_{-\infty}^{\infty} \phi(\omega) d\omega = \int_0^{\infty} \phi(\omega) d\omega \quad (8)$$

By definition $e^{-i\omega\tau} = \cos \omega\tau - i \sin \omega\tau$ the imaginary part vanishes due to symmetry.

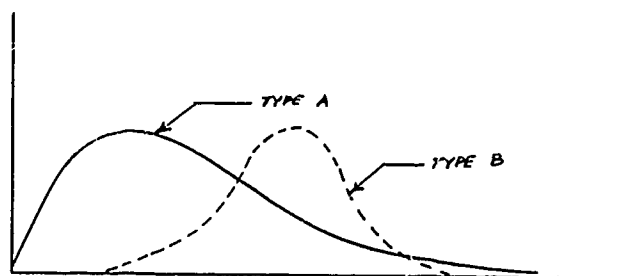
$$R(\tau) = \frac{1}{2} \int_{-\infty}^{\infty} \phi(\omega) \cos \omega\tau d\omega$$

By comparison with previous definitions

$$\phi(\omega) = \frac{1}{\pi} \int_{-\infty}^{\infty} R(\tau) \cos \omega\tau d\tau$$

It is quite evident that the power spectral density is a Fourier cosine transform of the auto-correlation function and for a random function this is quite significant since the auto-correlation function can be easily measured and more clearly understood.

Plotting $\phi(\omega)$ against ω produces a curve, the area under which represents the mean square of the random function as indicated in equation 8. The spectral character can appear either as a distributed form (type A) or as a dominant frequency (type B) or a combination of either. The figure below is in an approximate normalized form and illustrates the two types of responses.



UNCLASSIFIED
Security Classification

14. KEY WORDS	LINK A		LINK B		LINK C	
	ROLE	WT	ROLE	WT	ROLE	WT
Data Handling System						
Antenna Vibration						
Aeroelastic Model						

INSTRUCTIONS

1. **ORIGINATING ACTIVITY:** Enter the name and address of the contractor, subcontractor, grantee, Department of Defense activity or other organization (*corporate author*) issuing the report.

2a. **REPORT SECURITY CLASSIFICATION:** Enter the overall security classification of the report. Indicate whether "Restricted Data" is included. Marking is to be in accordance with appropriate security regulations.

2b. **GROUP:** Automatic downgrading is specified in DoD Directive 5200.10 and Armed Forces Industrial Manual. Enter the group number. Also, when applicable, show that optional markings have been used for Group 3 and Group 4 as authorized.

3. **REPORT TITLE:** Enter the complete report title in all capital letters. Titles in all cases should be unclassified. If a meaningful title cannot be selected without classification, show title classification in all capitals in parenthesis immediately following the title.

4. **DESCRIPTIVE NOTES:** If appropriate, enter the type of report, e.g., interim, progress, summary, annual, or final. Give the inclusive dates when a specific reporting period is covered.

5. **AUTHOR(S):** Enter the name(s) of author(s) as shown on or in the report. Enter last name, first name, middle initial. If military, show rank and branch of service. The name of the principal author is an absolute minimum requirement.

6. **REPORT DATE:** Enter the date of the report as day, month, year; or month, year. If more than one date appears on the report, use date of publication.

7a. **TOTAL NUMBER OF PAGES:** The total page count should follow normal pagination procedures, i.e., enter the number of pages containing information.

7b. **NUMBER OF REFERENCES:** Enter the total number of references cited in the report.

8a. **CONTRACT OR GRANT NUMBER:** If appropriate, enter the applicable number of the contract or grant under which the report was written.

8b, 8c, & 8d. **PROJECT NUMBER:** Enter the appropriate military department identification, such as project number, subproject number, system numbers, task number, etc.

9a. **ORIGINATOR'S REPORT NUMBER(S):** Enter the official report number by which the document will be identified and controlled by the originating activity. This number must be unique to this report.

9b. **OTHER REPORT NUMBER(S):** If the report has been assigned any other report numbers (*either by the originator or by the sponsor*), also enter this number(s).

10. **AVAILABILITY/LIMITATION NOTICES:** Enter any limitations on further dissemination of the report, other than those

imposed by security classification, using standard statements such as:

- (1) "Qualified requesters may obtain copies of this report from DDC."
- (2) "Foreign announcement and dissemination of this report by DDC is not authorized."
- (3) "U. S. Government agencies may obtain copies of this report directly from DDC. Other qualified DDC users shall request through _____."
- (4) "U. S. military agencies may obtain copies of this report directly from DDC. Other qualified users shall request through _____."
- (5) "All distribution of this report is controlled. Qualified DDC users shall request through _____."

If the report has been furnished to the Office of Technical Services, Department of Commerce, for sale to the public, indicate this fact and enter the price, if known.

11. **SUPPLEMENTARY NOTES:** Use for additional explanatory notes.

12. **SPONSORING MILITARY ACTIVITY:** Enter the name of the departmental project office or laboratory sponsoring (paying for) the research and development. Include address.

13. **ABSTRACT:** Enter an abstract giving a brief and factual summary of the document indicative of the report, even though it may also appear elsewhere in the body of the technical report. If additional space is required, a continuation sheet shall be attached.

It is highly desirable that the abstract of classified reports be unclassified. Each paragraph of the abstract shall end with an indication of the military security classification of the information in the paragraph, represented as (TS), (S), (C), or (U).

There is no limitation on the length of the abstract. However, the suggested length is from 150 to 225 words.

14. **KEY WORDS:** Key words are technically meaningful terms or short phrases that characterize a report and may be used as index entries for cataloging the report. Key words must be selected so that no security classification is required. Identifiers, such as equipment model designation, trade name, military project code name, geographic location, may be used as key words but will be followed by an indication of technical context. The assignment of links, roles, and weights is optional.